Modeling Flow in Naturally Fractured Reservoirs: Effect of Fracture Aperture Distribution on Dominant Sub-Network for Flow

J. Gong and W. R. Rossen

Department of Geoscience & Engineering, Delft University of Technology, Delft, the Netherlands

Abstract: Fracture network connectivity and aperture (or conductivity) distribution are two crucial features controlling the flow behavior of naturally fractured reservoirs. The effect of connectivity on flow properties is well documented. We focus here on the influence of fracture aperture distribution. We model a two-dimensional fractured reservoir in which the matrix is impermeable and the fractures are well-connected. The fractures obey a power-law length distribution, as observed in natural fracture networks. For the aperture distribution, since the information from subsurface fracture networks is limited, we test a number of cases: log-normal distributions (from narrow to broad), power-law distributions (from narrow to broad), and one case where the aperture is proportional to the fracture length. We find that even a well-connected fracture network can behave like a much sparser network when the aperture distribution is broad enough ($\alpha \leq 2$ for power-law aperture distributions and $\sigma \geq 0.4$ for log-normal aperture distributions). Specifically, most fractures can be eliminated leaving the remaining dominant sub-network with 90% of the permeability of the original fracture network. We determine how broad the aperture distribution must be to approach this behavior and the dependence of the dominant sub-network on the parameters of the aperture distribution. We also explore whether one can identify the dominant sub-network without doing flow calculations.

List of Figures and Tables

(c) α = 3, (d) α = 4, (e) α = 5, (f) α = 6. Results of one realization shown for each value of α.

- **Figure 11.** Standard deviation of apertures in the sub-network backbone (d_b^σ) normalized by the standard deviation of apertures in the original fracture network (d_o^σ), plotted against the length of the backbone of the truncated fracture network (l_b) normalized the total length of the original fracture network (l_o): power-law aperture distributions with (a) α = 1.001, (b) α = 2, (c) α = 3, (d) α = 4, (e) α = 5, (f) α = 6. Results of 100 realizations shown for each value of α. Red curve is the average trend curve.

- **Figure 12.** Average curves from Fig. 11.

- **Figure 13.** Minimum aperture of the sub-network backbone (d_b^m) normalized by the minimum aperture of the original fracture network (d_o^m), plotted against the length of backbone of the truncated fracture network (l_b) normalized by the total length of the original fracture network (l_o): power-law aperture distributions with (a) α = 1.001, (b) α = 2, (c) α = 3, (d) α = 4, (e) α = 5, (f) α = 6. Results of 100 realizations shown for each value of α. Red curve is the average trend curve.

- **Figure 14.** Average curves from Fig. 13.

- **Figure 15.** Average aperture of the sub-network backbone (d_b^μ) normalized by the average aperture of the original fracture network (d_o^μ), plotted against the length of the backbone of the truncated fracture network (l_b) normalized the total length of the original fracture network (l_o): power-law aperture distributions with (a) α = 1.001, (b) α = 2, (c) α = 3, (d) α = 4, (e) α = 5, (f) α = 6. Results of 100 realizations shown for each value of α. Red curve is the average trend curve.

- **Figure 16.** Average curves from Fig. 15.

- **Figure 17.** Fracture aperture follows log-normal distribution with the same mean value but different standard deviation in log-10 space.

- **Figure 18.** Sub-network equivalent permeability (K) normalized by the equivalent permeability of the original fracture network (K_0), plotted against the length of the backbone of the truncated fracture network (l_b) normalized by the total length of the original fracture network (l_o): log-normal aperture distributions with (a) σ = 0.1, (b) σ = 0.2, (c) σ = 0.3, (d) σ = 0.4, (e) σ = 0.5, (f) σ = 0.6. Results of 100 realizations shown for each value of σ. Red curve is the average trend curve.

- **Figure 19.** Average curves from Fig. 18.

- **Figure 20.** Original fracture network and the backbone of the sub-network which retains 90% of the original equivalent network permeability, for log-normal aperture distribution: (a) original fracture network. (b)- (g) sub-network which retains 90% of the original network permeability: log-normal aperture distribution with (a) σ = 0.1, (b) σ = 0.2, (c) σ = 0.3, (d) σ = 0.4, (e) σ = 0.5, (f) σ = 0.6. One realization shown for each value of σ.

- **Figure 21.** Length of sub-network backbone (l_b) normalized by the total length of the original fracture network (l_o) plotted against the percentage of eliminated fractures, for the cases of log-normal aperture distributions with the same log-mean value but different log-standard deviations (σ) from 0.1 to 0.6. Average trend curve for 100 realizations shown for each value of σ.

- **Figure 22.** Histogram of *Q* for each fracture normalized by the minimum value of *Q* for all fractures in the backbone in log-10 space: log-normal aperture distributions with (a) σ = 0.1, (b) σ = 0.2, (c) σ = 0.3, (d) σ = 0.4, (e) σ = 0.5, (f) σ = 0.6. Results of one realization shown for each value of σ.

- **Figure 23.** *Q* for each fracture normalized by the minimum value of *Q* for all the fractures in log-10 space plotted against fracture aperture: log-normal aperture distributions with (a) σ = 0.1, (b) σ = 0.2, (c) σ = 0.3, (d) σ = 0.4, (e) σ = 0.5, (f) σ = 0.6. Results of one realization shown for each value of σ.

- **Figure 24.** *Q* for each fracture normalized by the minimum value of *Q* for all the fractures in log-10 space plotted against fracture length *l*: log-normal aperture distributions with (a) σ = 0.1, (b) σ = 0.2, (c) σ = 0.3, (d) σ = 0.4, (e) σ = 0.5, (f) σ = 0.6. Results of one realization shown for each value of σ.

- **Figure 25.** Comparison of *Q* of fractures when they are in the original fracture network (Q_0) and in the critical sub-network (Q_b): log-normal aperture distributions with (a) σ = 0.1, (b) σ = 0.2, (c) σ = 0.3, (d) σ = 0.4, (e) σ = 0.5, (f) σ = 0.6. Both of Q_0 and Q_b are normalized by the minimum value of *Q* in the original fracture network (Q_o^m). Results of one realization shown for each value of σ.

- **Figure 26.** Comparison of aperture distribution of the original fracture network and the critical sub-network: log-normal aperture distributions with (a) σ = 0.1, (b) σ = 0.2, (c) σ = 0.3, (d) σ = 0.4, (e) σ = 0.5, (f) σ = 0.6. Results of one realization shown for each value of σ.

- **Figure 27.** Standard deviation of apertures in the sub-network backbone (d_b^σ) normalized by the standard deviation of apertures in the original backbone (d_o^σ), plotted against the length of the backbone of the truncated fracture network (l_b) normalized by the total length of the original fracture network (l_o): log-normal aperture distributions with (a) σ = 0.1, (b) σ = 0.2, (c) σ = 0.3, (d) σ = 0.4, (e) σ = 0.5, (f) σ = 0.6. Results of 100 realizations shown for each value of σ. Red curve is the average trend curve.

- **Figure 28.** Average curves from Fig. 27.

- **Figure 29.** Minimum aperture of the sub-network backbone (d_b^m) normalized by the minimum aperture of the original fracture network (d_o^m), plotted against the length of the backbone of the truncated fracture network (l_b) normalized by the total length of the original fracture network (l_o): log-normal aperture distributions with (a) σ = 0.1, (b) σ = 0.2, (c) σ = 0.3, (d) σ = 0.4, (e) σ = 0.5, (f) σ = 0.6. Results for 100 realizations shown for each value of σ. Red curve is the average trend curve.

- **Figure 30.** Average curves from Fig. 29.

- **Figure 31.** Average aperture of the sub-network backbone (d_b^m) normalized by the average aperture of the original fracture network (d_o^m), plotted against the length of backbone of the truncated fracture network (l_b) normalized by the total length of the original fracture network (l_o): log-normal aperture distributions with (a) σ = 0.1, (b) σ = 0.2, (c) σ = 0.3, (d) σ = 0.4, (e) σ = 0.5, (f) σ = 0.6. Results of 100 realizations shown for each value of σ. Red curve is the average trend curve.

- **Figure 32.** Average curves from Fig. 31.

- **Figure 33.** Sub-network equivalent permeability (K) normalized by the equivalent permeability of the original fracture network (K_0), plotted against the length of the backbone of the truncated fracture network (l_b) normalized by the total length of the original fracture network (l_0): aperture is proportional to fracture length. Results of 100 realizations shown. Red curve is the average trend curve.

- **Figure 34.** Average curves from Fig. 2b and Fig. 33.

- **Figure 35.** Histogram of Q of each fracture normalized by the minimum value of Q of all the fractures in log-10 space: aperture is proportional to fracture length. Results of one realization shown.

- **Figure 36.** Q of each fracture normalized by the minimum value of Q of all the fractures in log-10 space plotted against aperture: aperture is proportional to fracture length. Results of one realization shown.

- **Figure 37.** Comparison of aperture distributions of the original fracture network and the critical sub-network: aperture is proportional to fracture length. Results of one realization shown.

- **Figure 38.** Comparison of Q of fractures when they are in the original fracture network (Q_0) and in the critical sub-network (Q_b): the case of the aperture is proportional to the fracture length. Both of Q_0 and Q_b are normalized by the minimum value of Q in the original fracture network (Q_o^m). Results of one realization shown.

- **Figure 39.** Standard deviation of apertures in the critical sub-network backbone (d_b^σ) normalized by the standard deviation of apertures in the original fracture network (d_o^σ), plotted against the length of the backbone of the truncated fracture network (l_b) normalized by the total length of the original fracture network (l_0): aperture is proportional to fracture length. Results of 100 realizations shown. Red curve is the average trend curve.

- **Figure 40.** Minimum aperture of the sub-network backbone (d_b^m) normalized by the minimum aperture of the original fracture network (d_o^m)), plotted against the length of the backbone of the truncated fracture network (l_b) normalized by the total length of the original fracture network (l_0): aperture is proportional to fracture length. Results of 100 realizations shown. Red curve is the average trend curve.

- **Figure 41.** Average aperture of the sub-network backbone (d_b^{μ}) normalized by the average aperture of the original fracture network (d_o^{μ}), plotted against the length of the backbone of the truncated fracture network (l_b) normalized by the total length of the original fracture network (l_o): aperture is proportional to fracture length. Results of 100 realizations shown. Red curve is the average trend curve.

- **Figure 42.** Sub-network equivalent permeability (K) normalized by the equivalent permeability of the original fracture network (K_0), plotted against the length of the backbone of the truncated fracture network (l_b) normalized by the total length of the original fracture network (l_o) for power-law aperture distributions with (a) α = 1.001, (b) α = 2, (c) α = 6. Fractures are eliminated according to different criteria.

- **Figure 43.** Sub-network equivalent permeability (K) normalized by the equivalent permeability of the original fracture network (K_0), plotted against the length of the backbone of the truncated fracture network (l_b) normalized by the total length of the original fracture network (l_o) for log-normal aperture distributions with (a) σ = 0.1, (b) σ = 0.2, (c) σ = 0.6. Fractures are eliminated according to different criteria.

- **Figure 44.** Sub-network equivalent permeability (K) normalized by the equivalent permeability of the original fracture network (K_0), plotted against the length of the backbone of the truncated fracture network (l_b) normalized by the total length of the original fracture network (l_o), for the cases where the aperture is proportional to the fracture length. Fractures are eliminated according to different criteria.

- **Table 1.** Description of criterion.

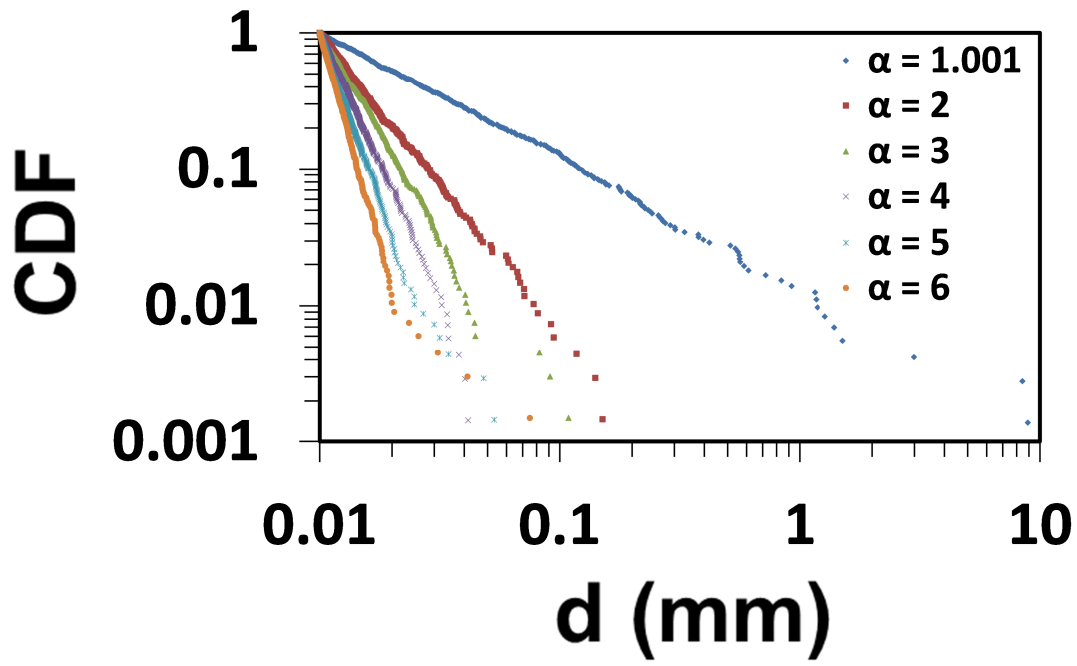

Figure 1. Fracture aperture d for one realization of a power-law distribution for each value of the exponent α.

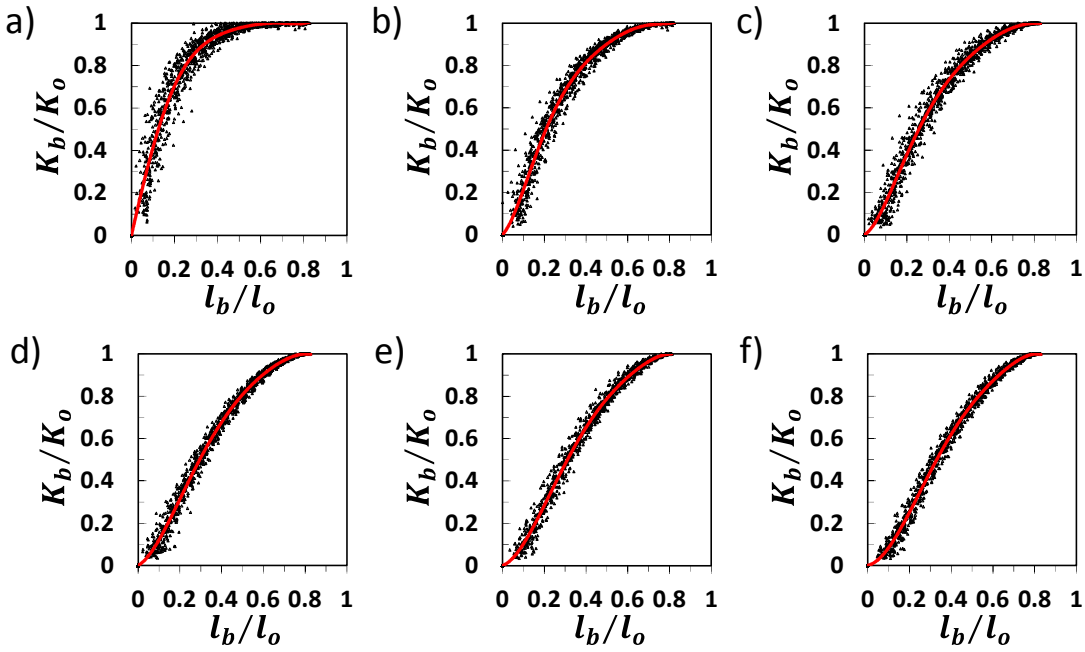

Figure 2. Sub-network equivalent permeability (K) normalized by the equivalent permeability of the original fracture network (K_0), plotted against the length of the backbone of the truncated fracture network (l_b) normalized by the total length of the original fracture network (l_o): power law aperture distributions with (a) α = 1.001, (b) α = 2, (c) α = 3, (d) α = 4, (e) α = 5, (f) α = 6. Results of 100 realizations shown for each value of α. Red curve is the average trend curve.

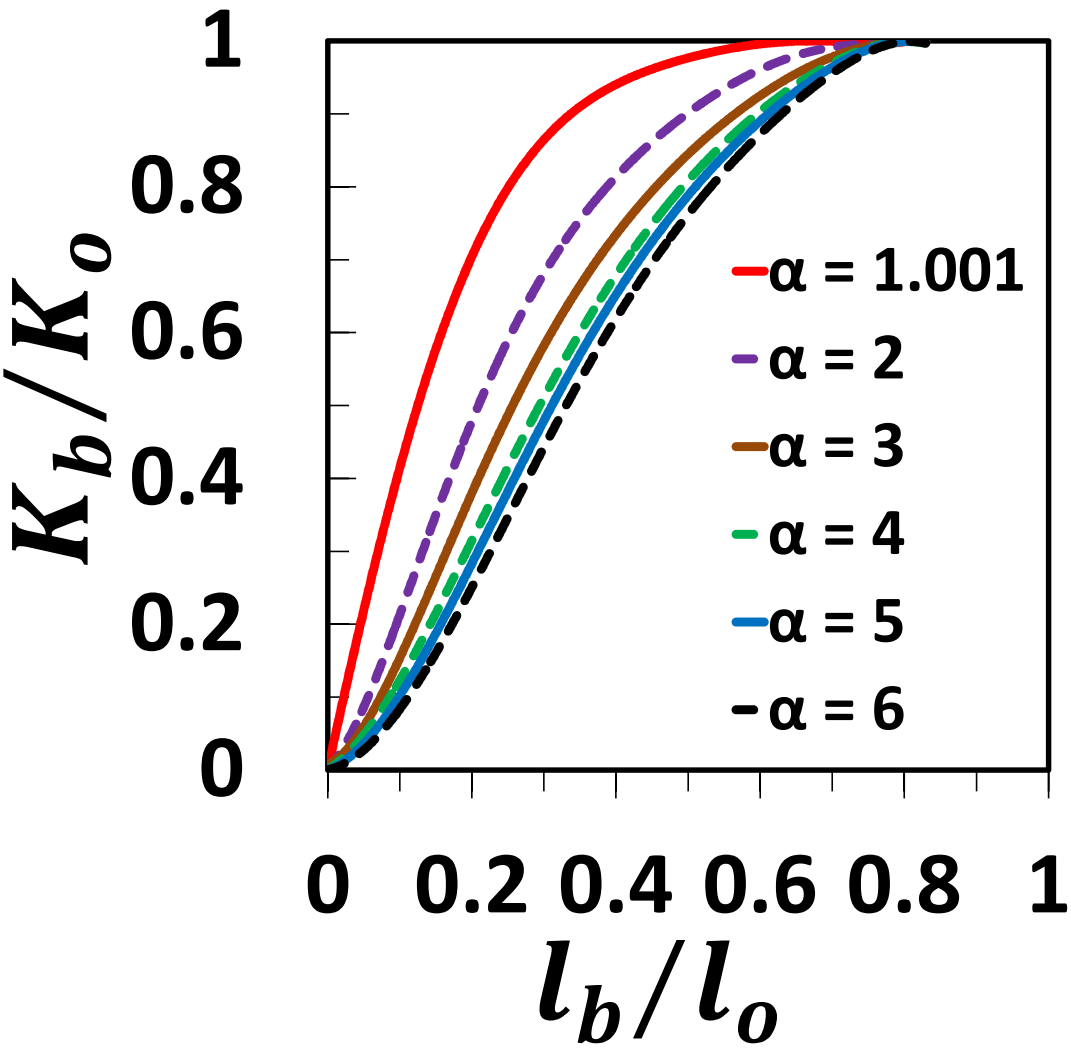

Figure 3. Average curves from Fig.2.

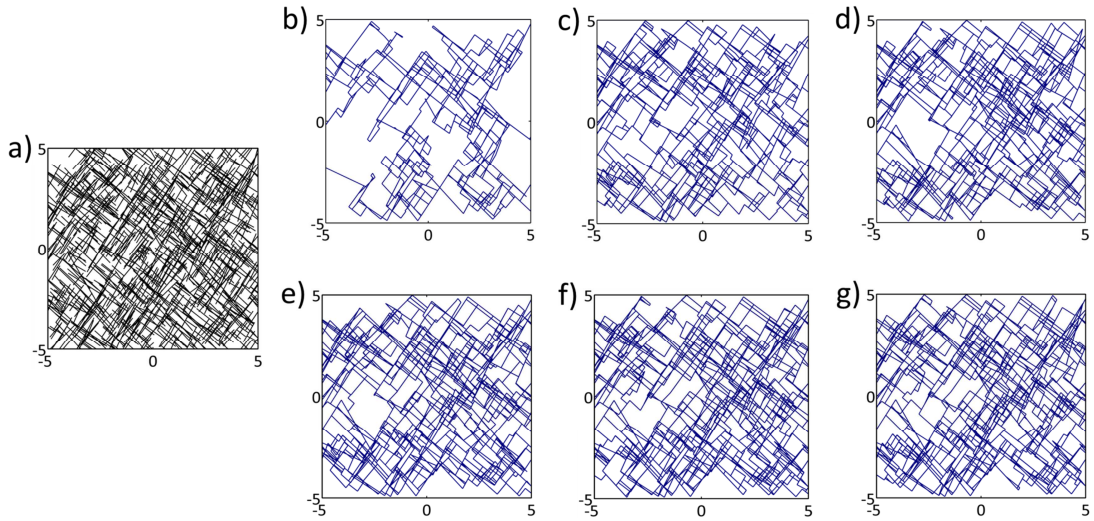

Figure 4. Original fracture network and backbone of the sub-network which retains 90% of the original equivalent network permeability: (a) original fracture network. (b-g) sub-network which retains 90% of the original network permeability: power-law aperture distribution with (b) α = 1.001, (c) α = 2, (d) α = 3, (e) α = 4, (f) α = 5, (g) α = 6. One realization shown for each value of α.

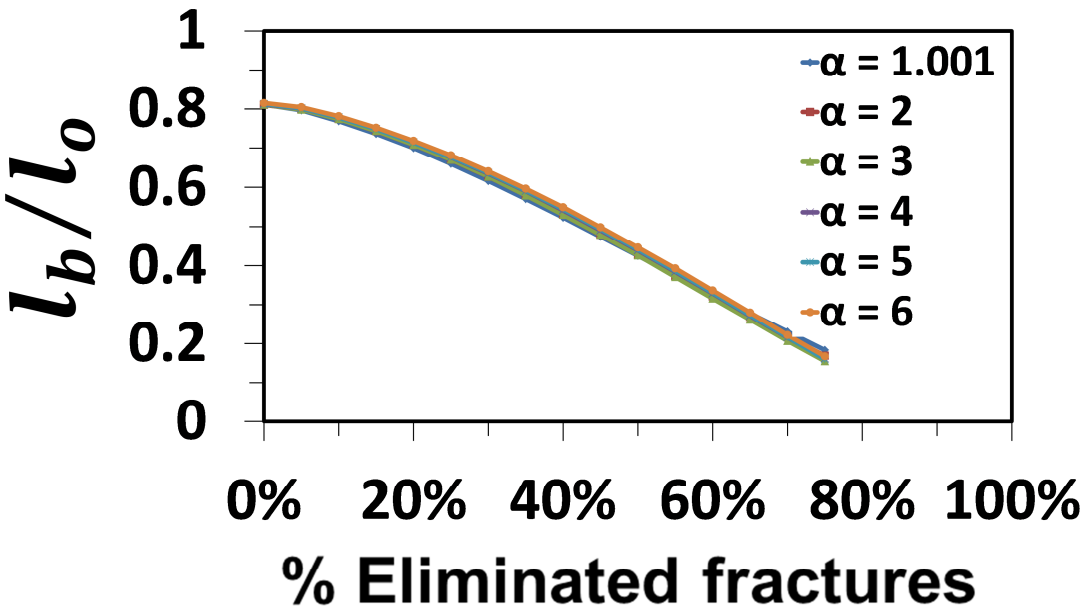

Figure 5. Length of the backbone of the truncated fracture network (l_b) normalized by the total length of the original fracture network (l_o) plotted against percentage of eliminated fractures, for power-law aperture distributions with exponent α = 1.001 to 6. Average trend curve for 100 realizations shown for each value of α.

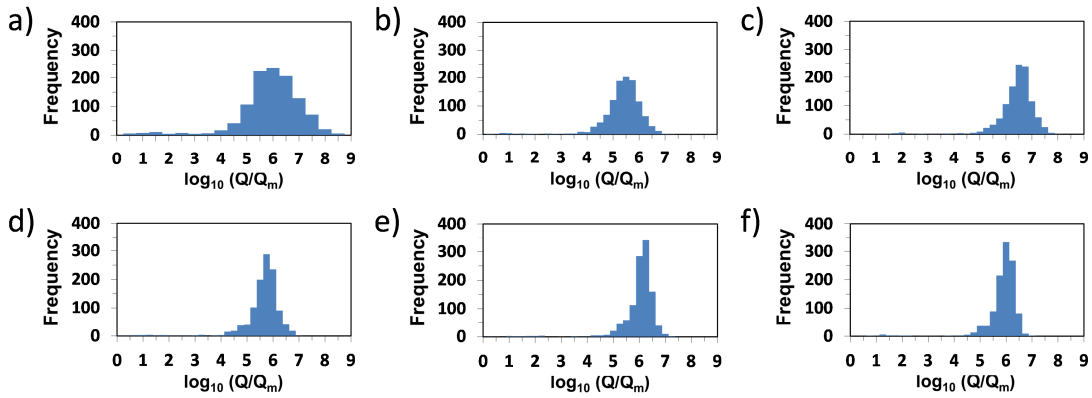

Figure 6. Histogram of Q for each fracture normalized by the minimum value of Q for all fractures in the backbone (Q_m) in log-10 space: power-law aperture distributions with (a) α = 1.001, (b) α = 2, (c) α = 3, (d) α = 4, (e) α = 5, (f) α = 6. Results of one realization shown for each value of α.

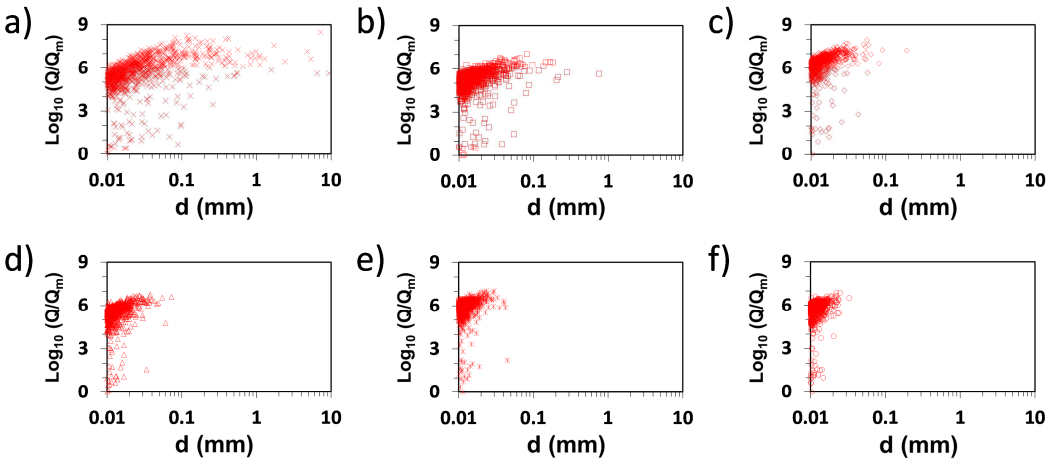

Figure 7. *Q* for each fracture normalized by the minimum value of *Q* for all the fractures in log-10 space against the aperture d: power-law aperture distributions with (a) α = 1.001, (b) α = 2, (c) α = 3, (d) α = 4, (e) α = 5, (f) α = 6. Results of one realization shown for each value of α.

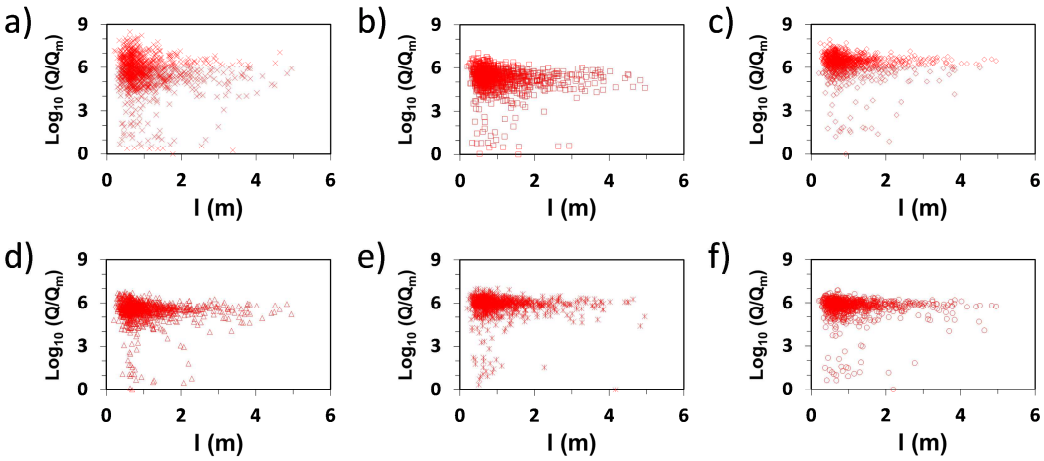

Figure 8. *Q* of each fracture normalized by the minimum value of *Q* in log-10 space against the fracture length *l*: power-law aperture distributions with (a) α = 1.001, (b) α = 2, (c) α = 3, (d) α = 4, (e) α = 5, (f) α = 6. Results of one realization shown for each value of α.

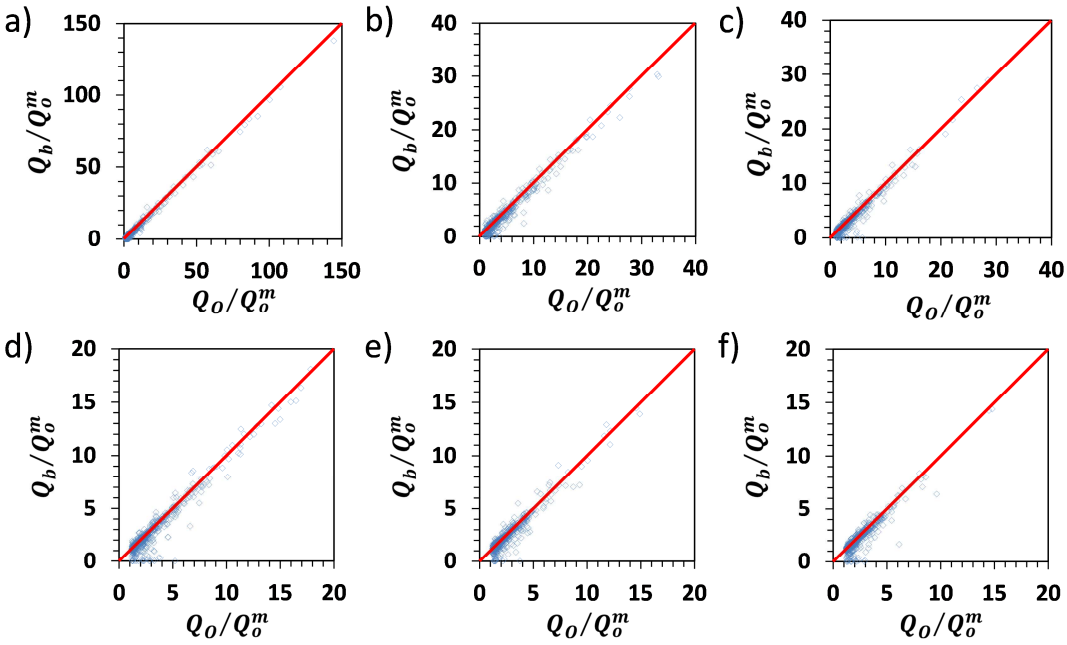

Figure 9. Comparison of Q for fractures in the original fracture network (Q_0) and in the critical sub-network (Q_b): power-law aperture distributions with (a) α = 1.001, (b) α = 2, (c) α = 3, (d) α = 4, (e) α = 5, (f) α = 6. Both of Q_0 and Q_b are normalized by the minimum value of Q in the original fracture network (Q_o^m). Results of one realization shown for each value of α.

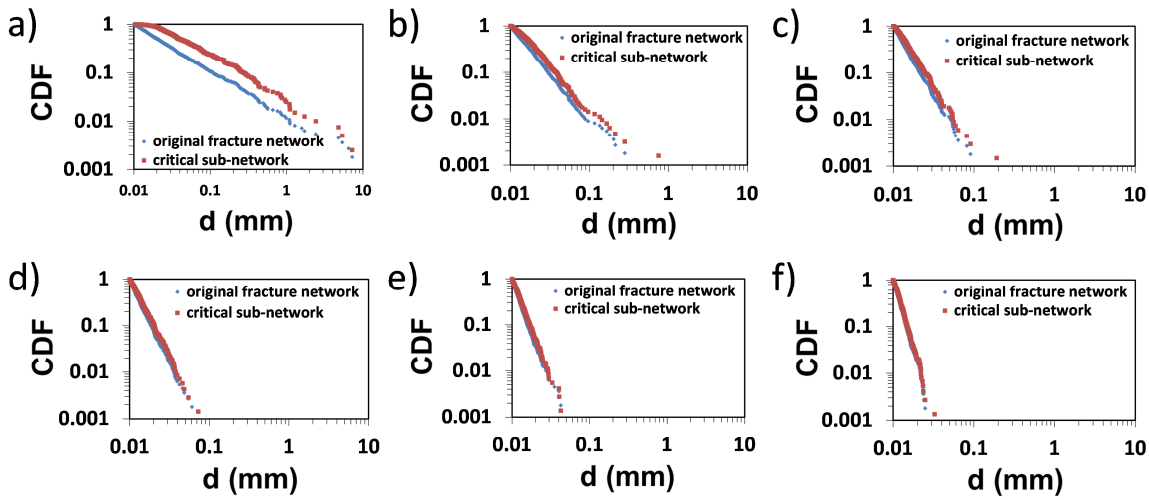

Figure 10. Comparison of the aperture distribution of the original fracture network and the critical sub-network: power-law aperture distributions with (a) α = 1.001, (b) α = 2, (c) α = 3, (d) α = 4, (e) α = 5, (f) α = 6. Results of one realization shown for each value of α.

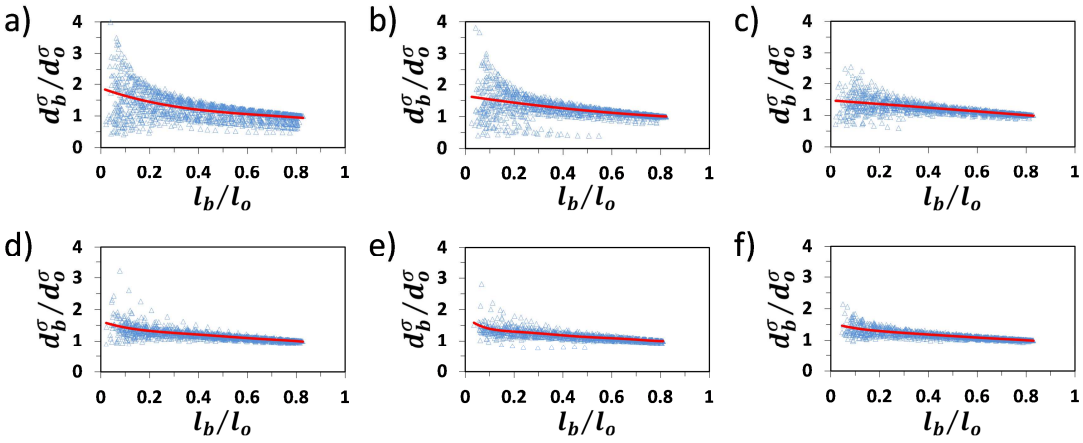

Figure 11. Standard deviation of apertures in the sub-network backbone (d_b^σ) normalized by the standard deviation of apertures in the original fracture network (d_o^σ), plotted against the length of the backbone of the truncated fracture network (l_b) normalized the total length of the original fracture network (l_o): power-law aperture distributions with (a) α = 1.001, (b) α = 2, (c) α = 3, (d) α = 4, (e) α = 5, (f) α = 6. Results of 100 realizations shown for each value of α. Red curve is the average trend curve.

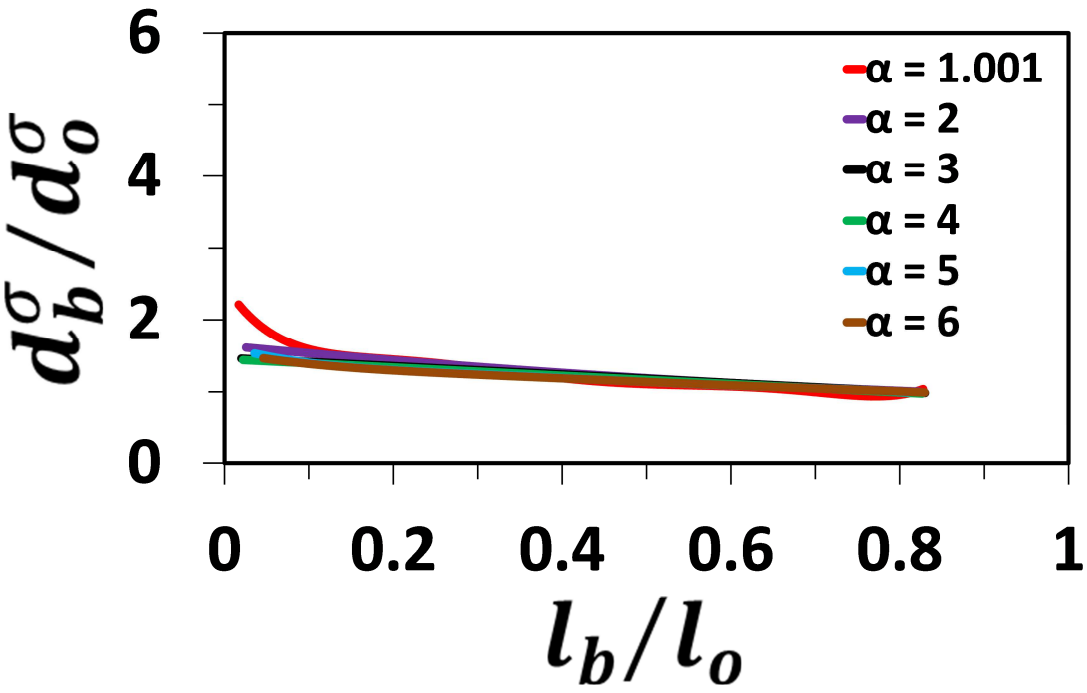

Figure 12. Average curves from Fig. 11.

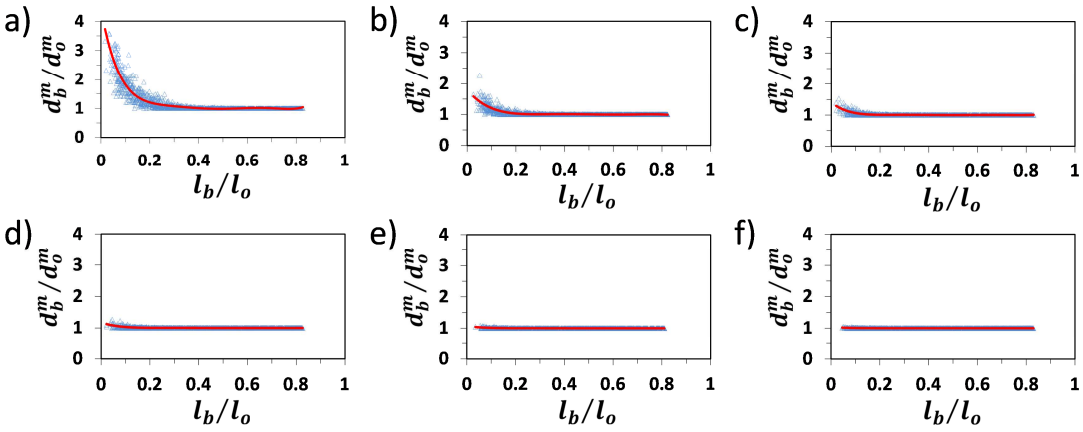

Figure 13. Minimum aperture of the sub-network backbone (d_b^m) normalized by the minimum aperture of the original fracture network (d_o^m), plotted against the length of backbone of the truncated fracture network (l_b) normalized by the total length of the original fracture network (l_o): power-law aperture distributions with (a) α = 1.001, (b) α = 2, (c) α = 3, (d) α = 4, (e) α = 5, (f) α = 6. Results of 100 realizations shown for each value of α. Red curve is the average trend curve.

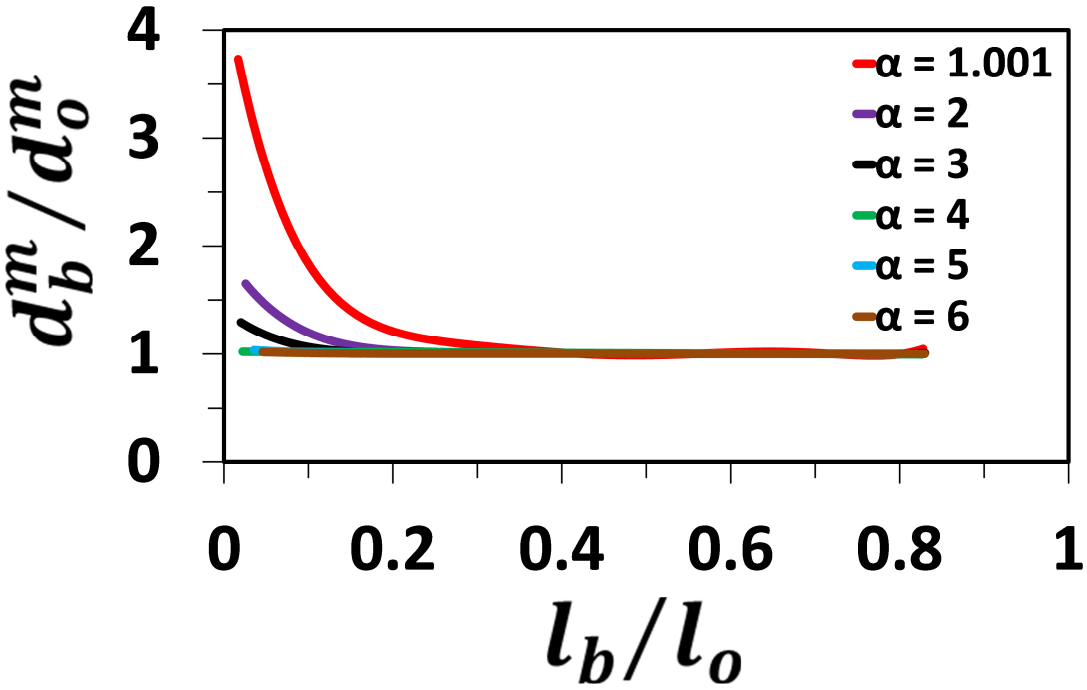

Figure 14. Average curves from Fig. 13.

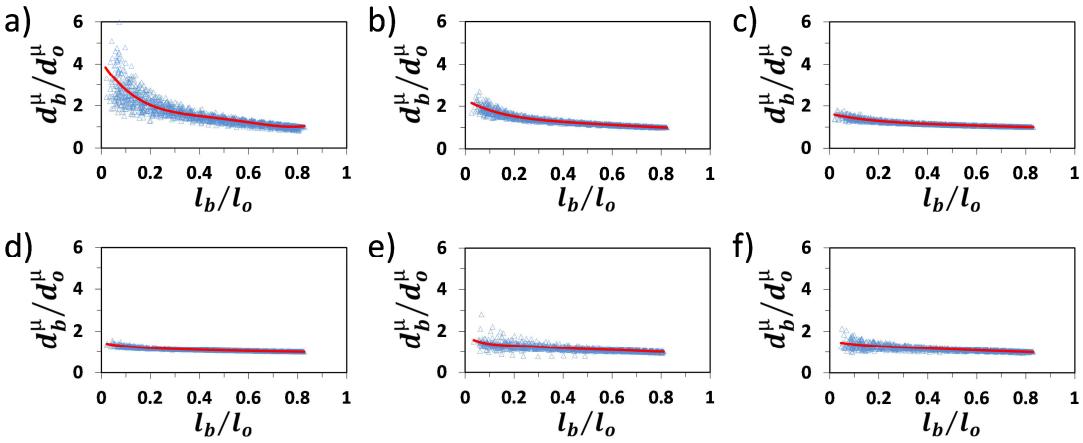

Figure 15. Average aperture of the sub-network backbone (d_b^μ) normalized by the average aperture of the original fracture network (d_o^μ), plotted against the length of the backbone of the truncated fracture network (l_b) normalized the total length of the original fracture network (l_o): power-law aperture distributions with (a) α = 1.001, (b) α = 2, (c) α = 3, (d) α = 4, (e) α = 5, (f) α = 6. Results of 100 realizations shown for each value of α. Red curve is the average trend curve.

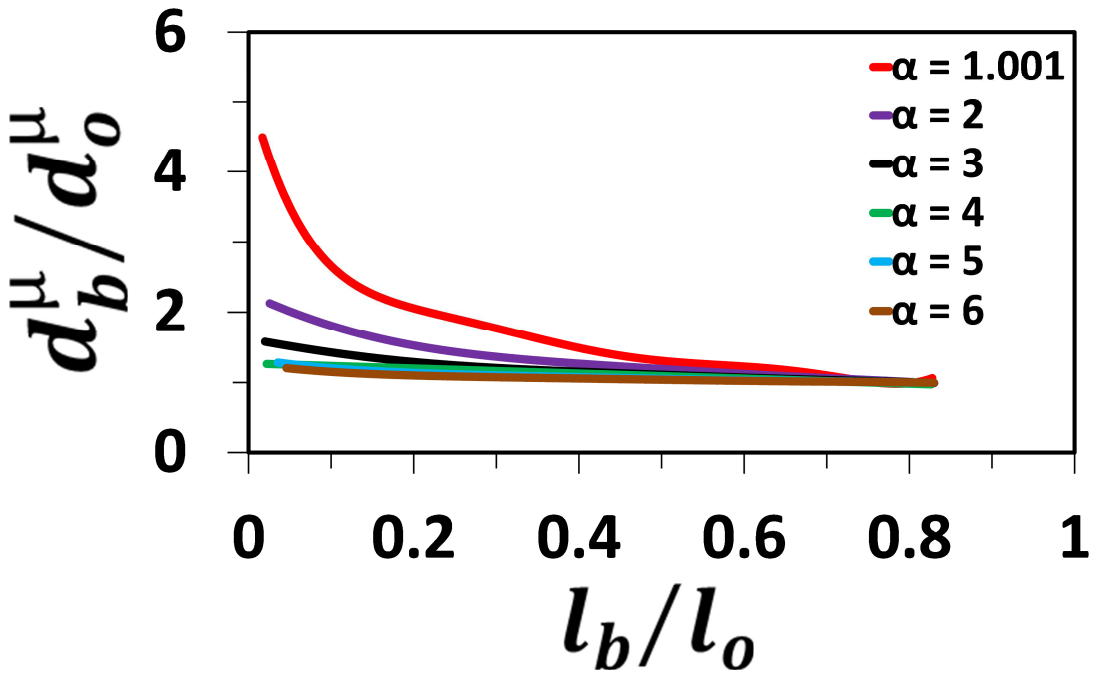

Figure 16. Average curves from Fig. 15.

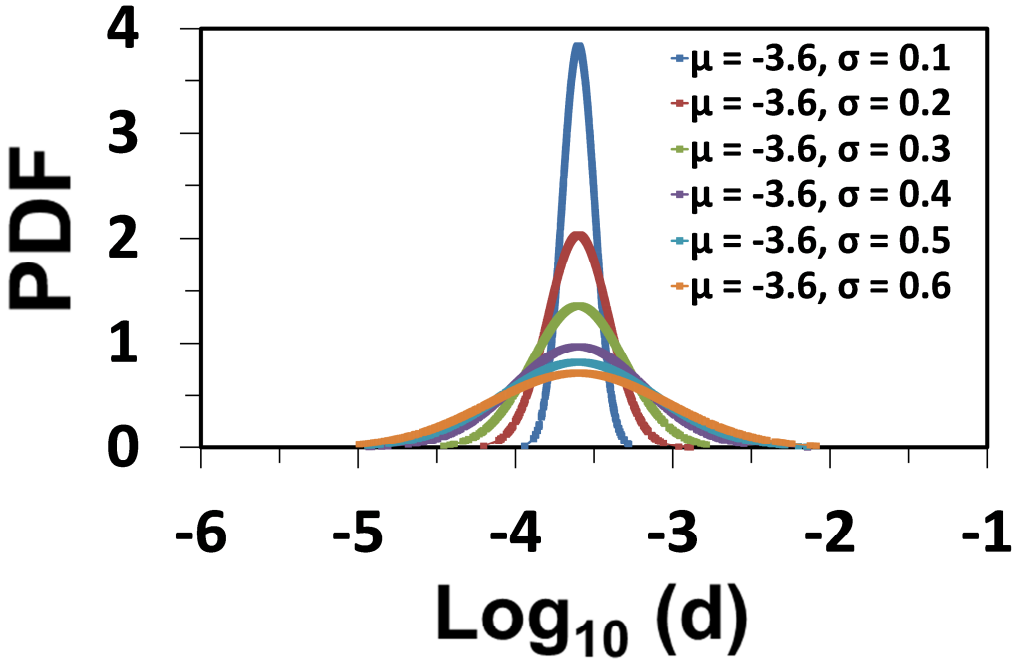

Figure 17. Fracture aperture follows log-normal distribution with the same mean value but different standard deviation in log-10 space.

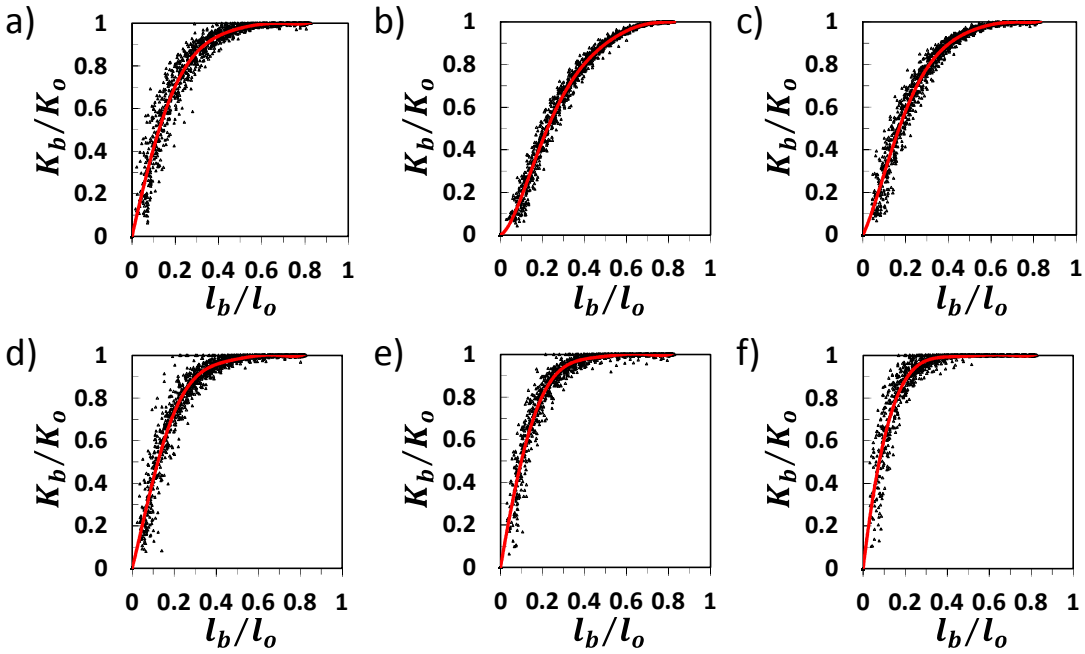

Figure 18. Sub-network equivalent permeability (K) normalized by the equivalent permeability of the original fracture network (K_0), plotted against the length of the backbone of the truncated fracture network (l_b) normalized by the total length of the original fracture network (l_o): log-normal aperture distributions with (a) σ = 0.1, (b) σ = 0.2, (c) σ = 0.3, (d) σ = 0.4, (e) σ = 0.5, (f) σ = 0.6. Results of 100 realizations shown for each value of σ. Red curve is the average trend curve.

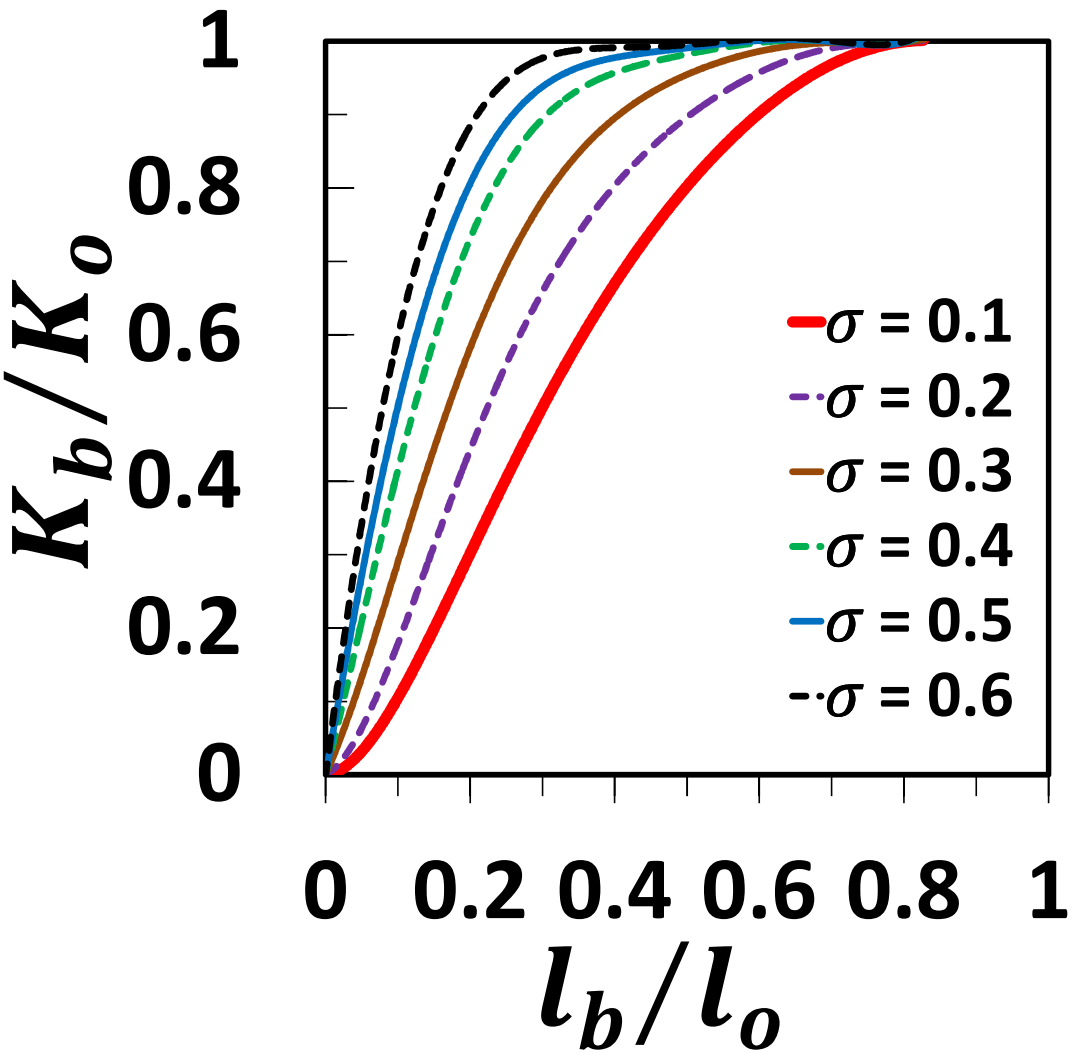

Figure 19. Average curves from Fig. 18.

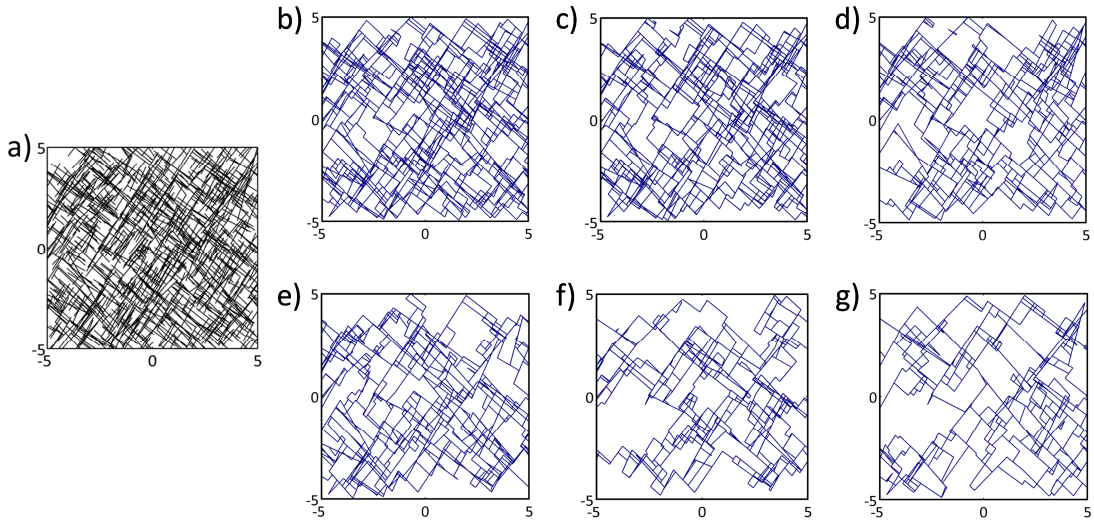

Figure 20. Original fracture network and the backbone of the sub-network which retains 90% of the original equivalent network permeability, for log-normal aperture distribution: (a) original fracture network. (b)- (g) sub-network which retains 90% of the original network permeability: log-normal aperture distribution with (a) σ = 0.1, (b) σ = 0.2, (c) σ = 0.3, (d) σ = 0.4, (e) σ = 0.5, (f) σ = 0.6. One realization shown for each value of σ.

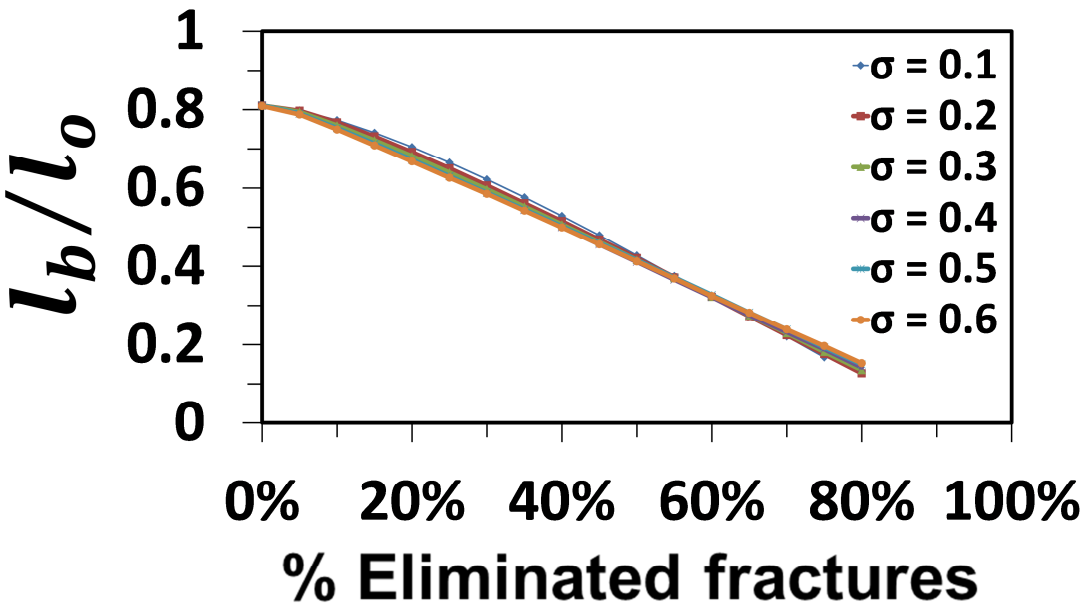

Figure 21. Length of sub-network backbone (l_b) normalized by the total length of the original fracture network (l_o) plotted against the percentage of eliminated fractures, for the cases of log-normal aperture distributions with the same log-mean value but different log-standard deviations (σ) from 0.1 to 0.6. Average trend curve for 100 realizations shown for each value of σ.

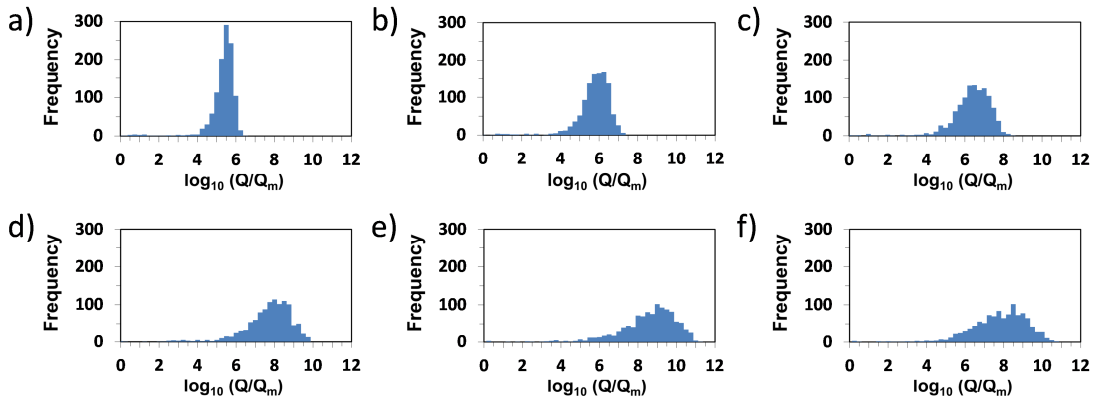

Figure 22. Histogram of Q for each fracture normalized by the minimum value of Q for all fractures in the backbone in log-10 space: log-normal aperture distributions with (a) σ = 0.1, (b) σ = 0.2, (c) σ = 0.3, (d) σ = 0.4, (e) σ = 0.5, (f) σ = 0.6. Results of one realization shown for each value of σ.

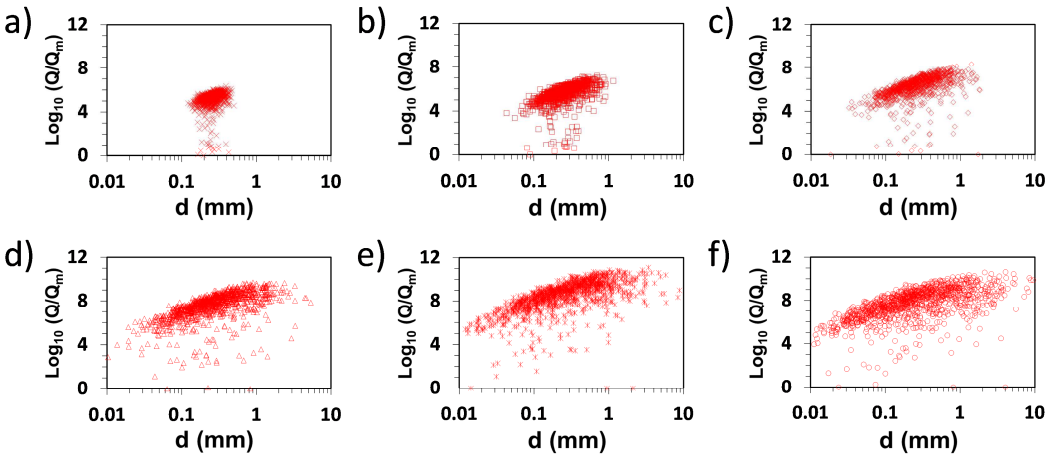

Figure 23. *Q* for each fracture normalized by the minimum value of *Q* for all the fractures in log-10 space plotted against fracture aperture: log-normal aperture distributions with (a) σ = 0.1, (b) σ = 0.2, (c) σ = 0.3, (d) σ = 0.4, (e) σ = 0.5, (f) σ = 0.6. Results of one realization shown for each value of σ.

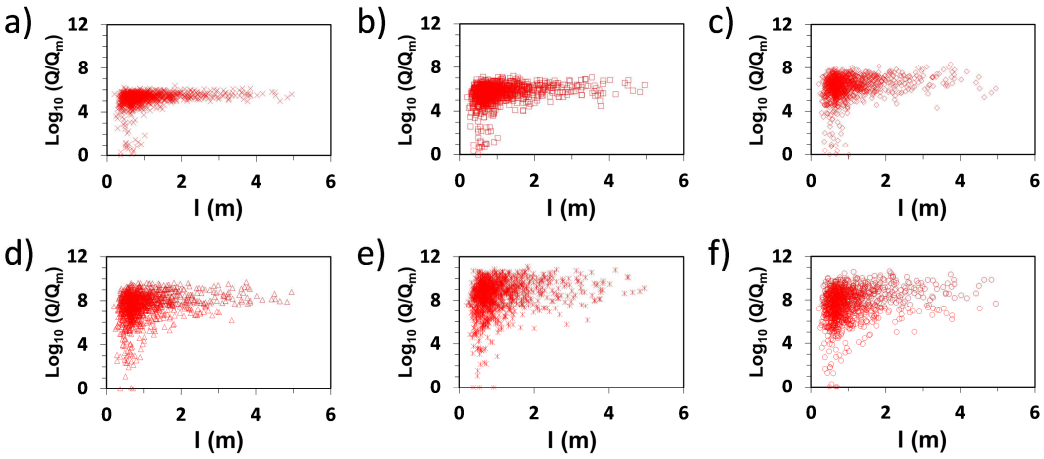

Figure 24. *Q* for each fracture normalized by the minimum value of *Q* for all the fractures in log-10 space plotted against fracture length l: log-normal aperture distributions with (a) σ = 0.1, (b) σ = 0.2, (c) σ = 0.3, (d) σ = 0.4, (e) σ = 0.5, (f) σ = 0.6. Results of one realization shown for each value of σ.

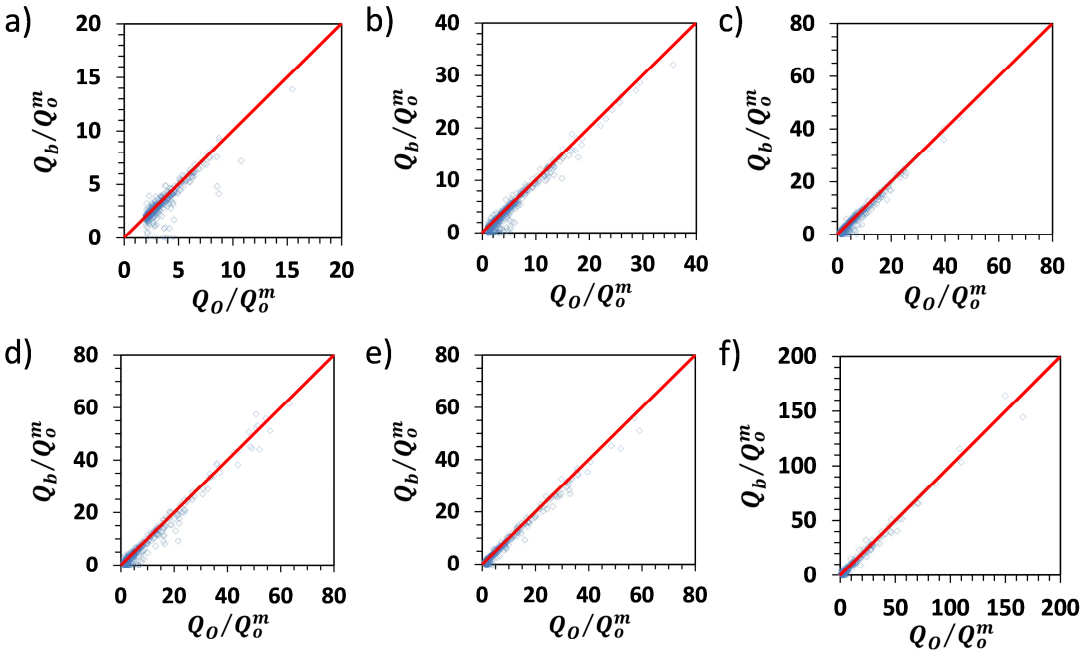

Figure 25. Comparison of Q of fractures when they are in the original fracture network (Q_0) and in the critical sub-network (Q_b): log-normal aperture distributions with (a) σ = 0.1, (b) σ = 0.2, (c) σ = 0.3, (d) σ = 0.4, (e) σ = 0.5, (f) σ = 0.6. Both of Q_0 and Q_b are normalized by the minimum value of Q in the original fracture network (Q_o^m). Results of one realization shown for each value of σ.

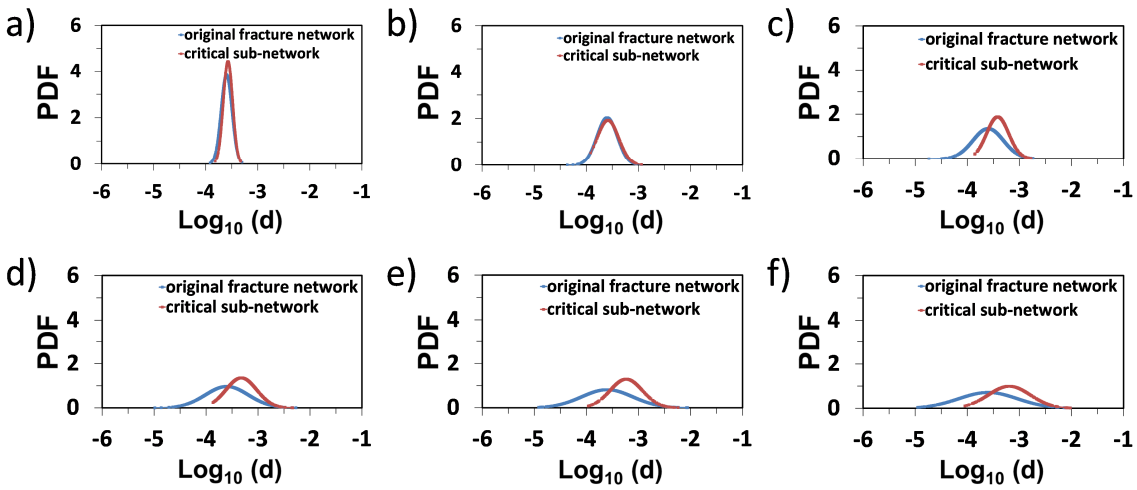

Figure 26. Comparison of aperture distribution of the original fracture network and the critical sub-network: log-normal aperture distributions with (a) σ = 0.1, (b) σ = 0.2, (c) σ = 0.3, (d) σ = 0.4, (e) σ = 0.5, (f) σ = 0.6. Results of one realization shown for each value of σ.

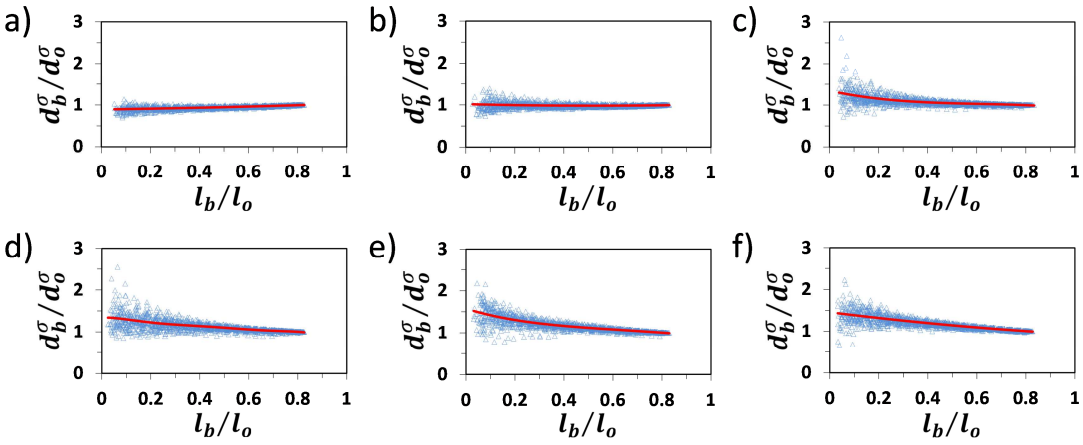

Figure 27. Standard deviation of apertures in the sub-network backbone (d_b^σ) normalized by the standard deviation of apertures in the original backbone (d_o^σ), plotted against the length of the backbone of the truncated fracture network (l_b) normalized by the total length of the original fracture network (l_o): log-normal aperture distributions with (a) σ = 0.1, (b) σ = 0.2, (c) σ = 0.3, (d) σ = 0.4, (e) σ = 0.5, (f) σ = 0.6. Results of 100 realizations shown for each value of σ. Red curve is the average trend curve.

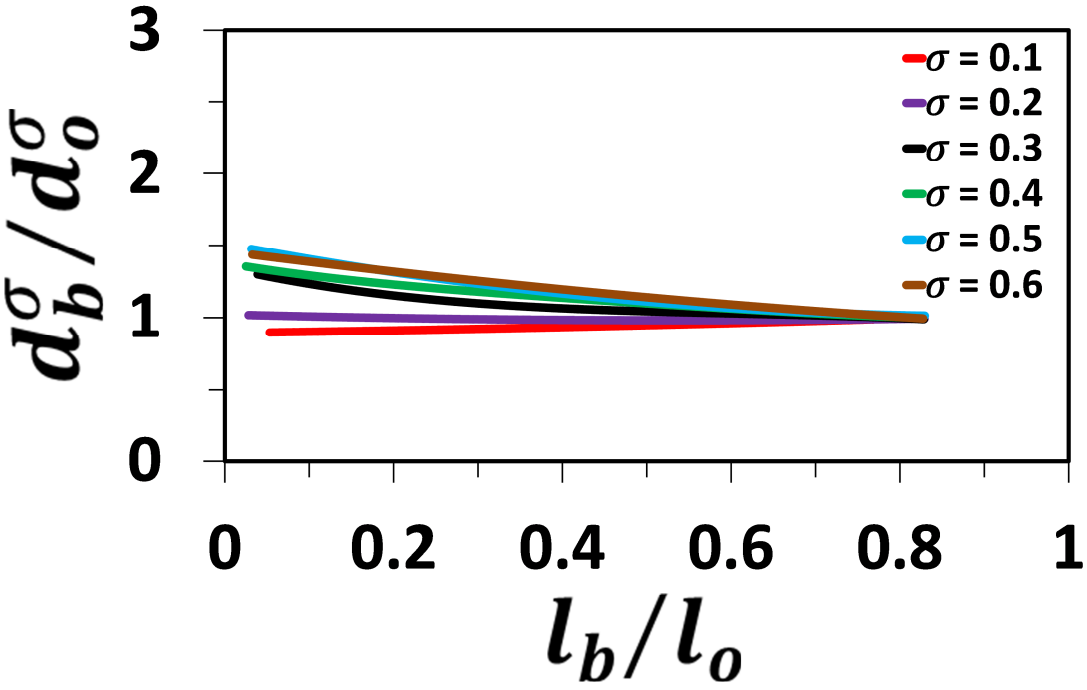

Figure 28. Average curves from Fig. 27.

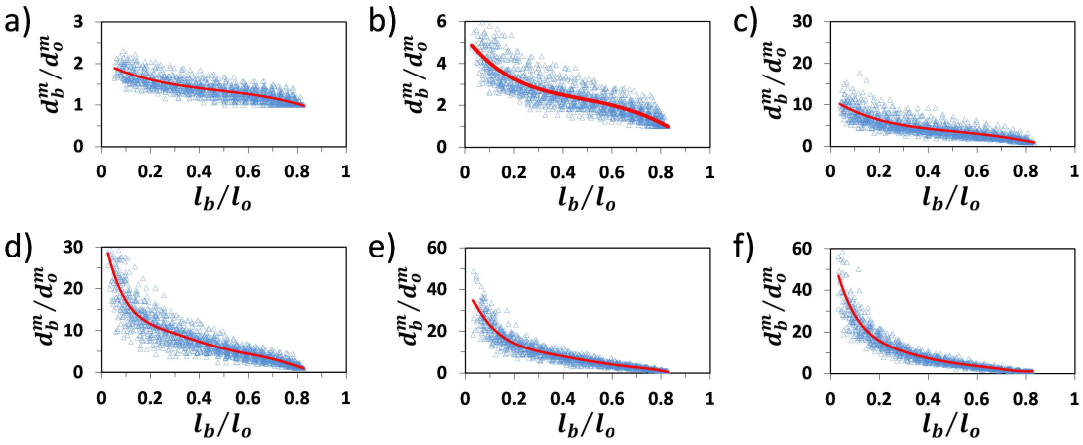

Figure 29. Minimum aperture of the sub-network backbone (d_b^m) normalized by the minimum aperture of the original fracture network (d_o^m), plotted against the length of the backbone of the truncated fracture network (l_b) normalized by the total length of the original fracture network (l_o): log-normal aperture distributions with (a) σ = 0.1, (b) σ = 0.2, (c) σ = 0.3, (d) σ = 0.4, (e) σ = 0.5, (f) σ = 0.6. Results for 100 realizations shown for each value of σ. Red curve is the average trend curve.

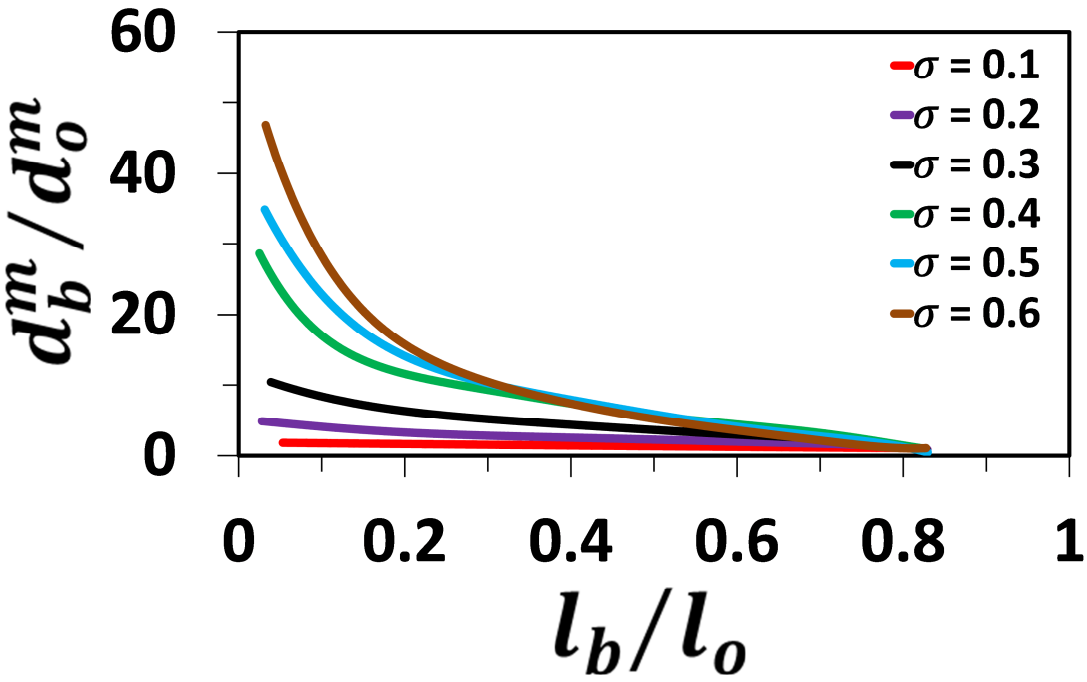

Figure 30. Average curves from Fig. 29.

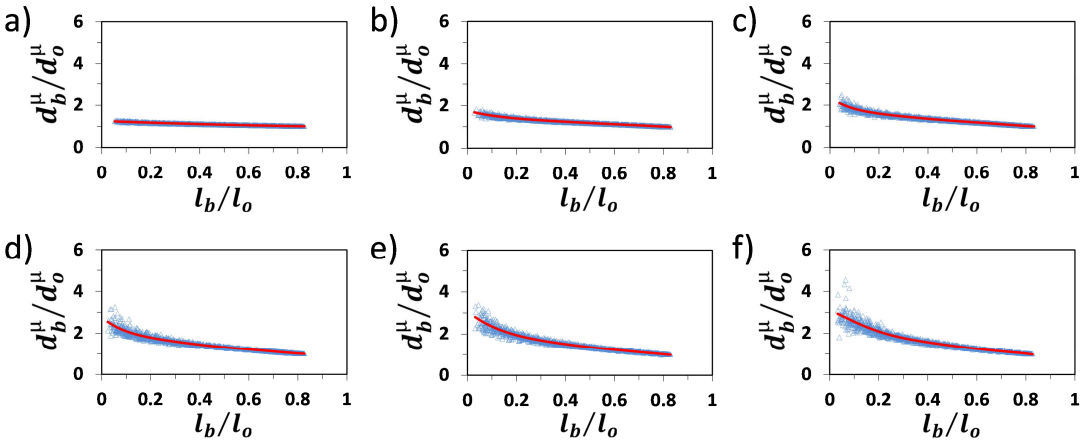

Figure 31. Average aperture of the sub-network backbone (d_b^m) normalized by the average aperture of the original fracture network (d_o^m), plotted against the length of backbone of the truncated fracture network (l_b) normalized by the total length of the original fracture network (l_o): log-normal aperture distributions with (a) σ = 0.1, (b) σ = 0.2, (c) σ = 0.3, (d) σ = 0.4, (e) σ = 0.5, (f) σ = 0.6. Results of 100 realizations shown for each value of σ. Red curve is the average trend curve.

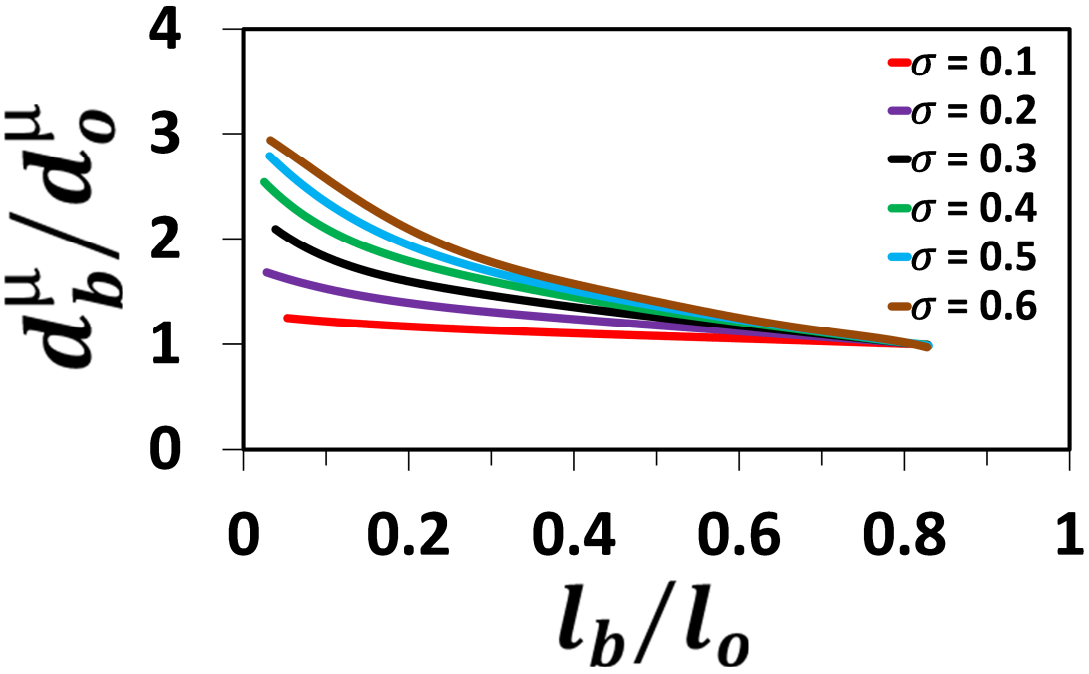

Figure 32. Average curves from Fig. 31.

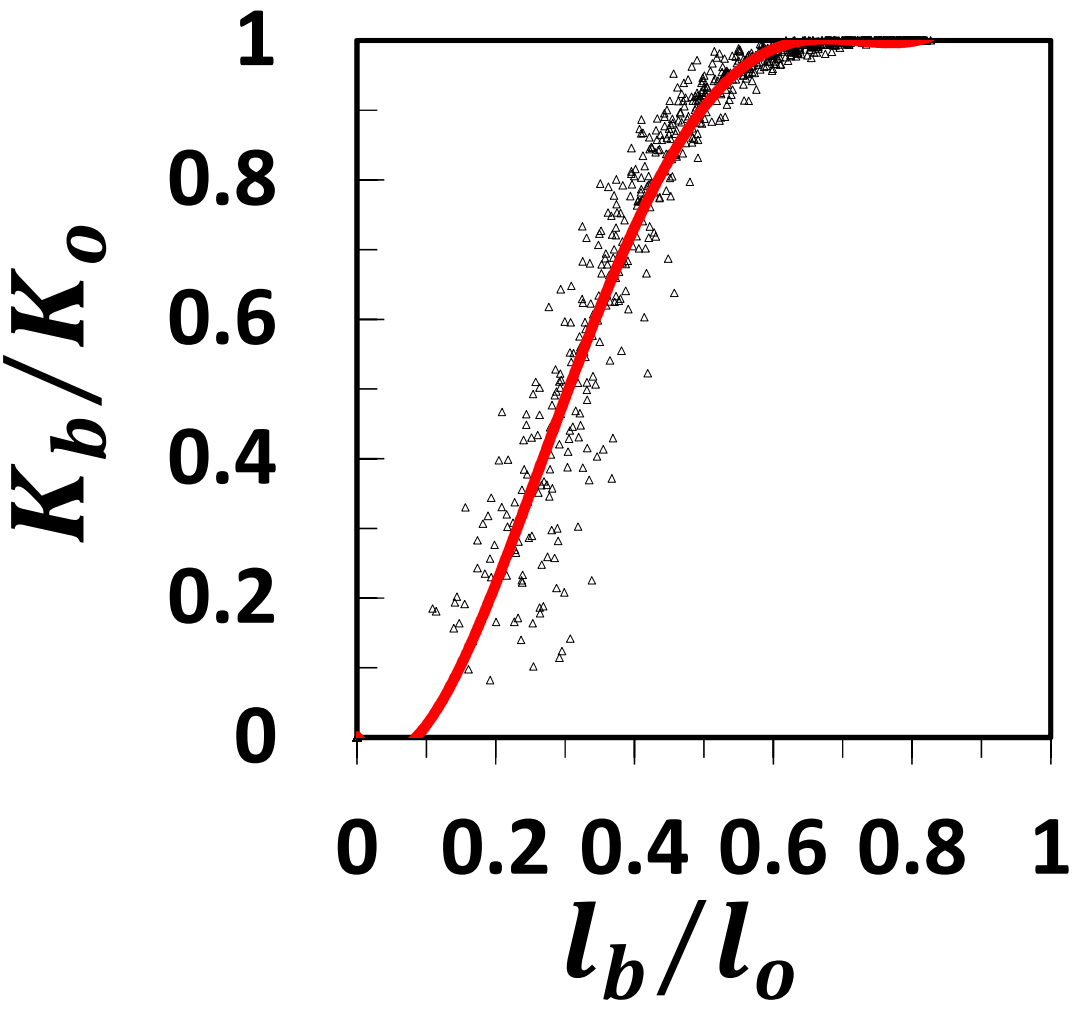

Figure 33. Sub-network equivalent permeability (K) normalized by the equivalent permeability of the original fracture network (K_0), plotted against the length of the backbone of the truncated fracture network (l_b) normalized by the total length of the original fracture network (l_0): aperture is proportional to fracture length. Results of 100 realizations shown. Red curve is the average trend curve.

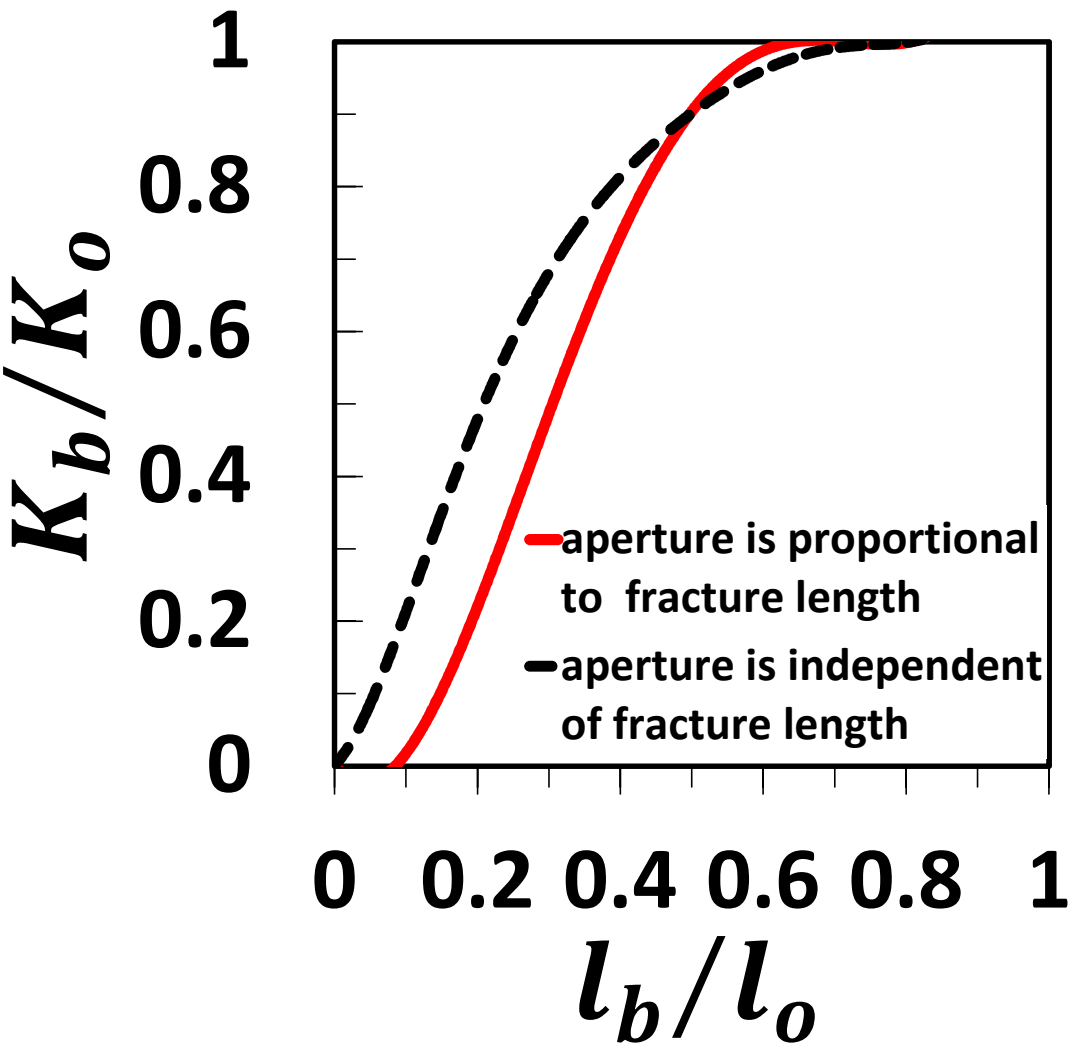

Figure 34. Average curves from Fig. 2b and Fig. 33.

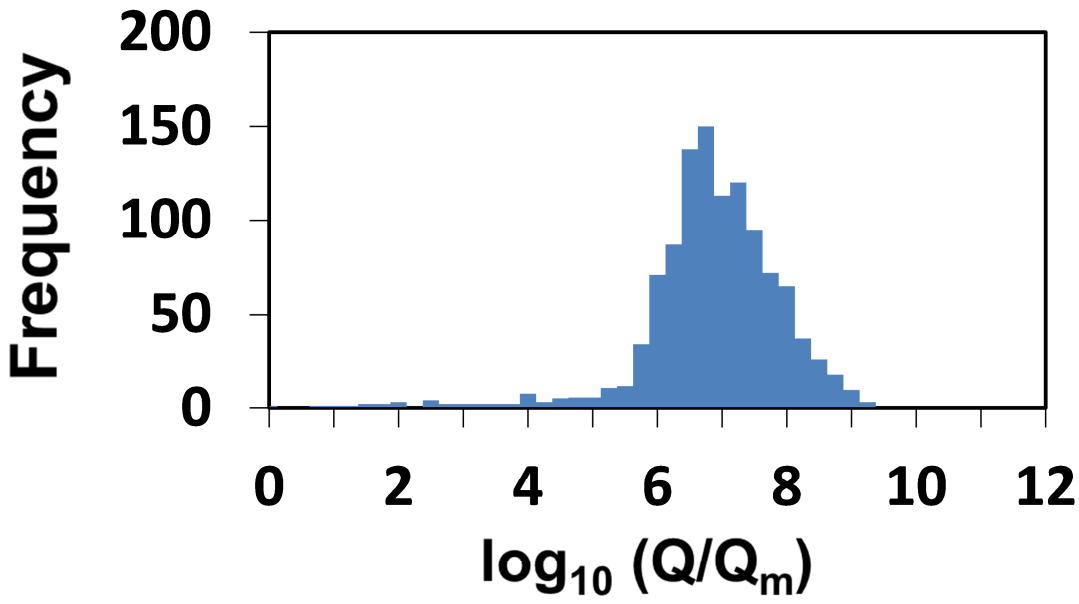

Figure 35. Histogram of *Q* of each fracture normalized by the minimum value of *Q* of all the fractures in log-10 space: aperture is proportional to fracture length. Results of one realization shown.

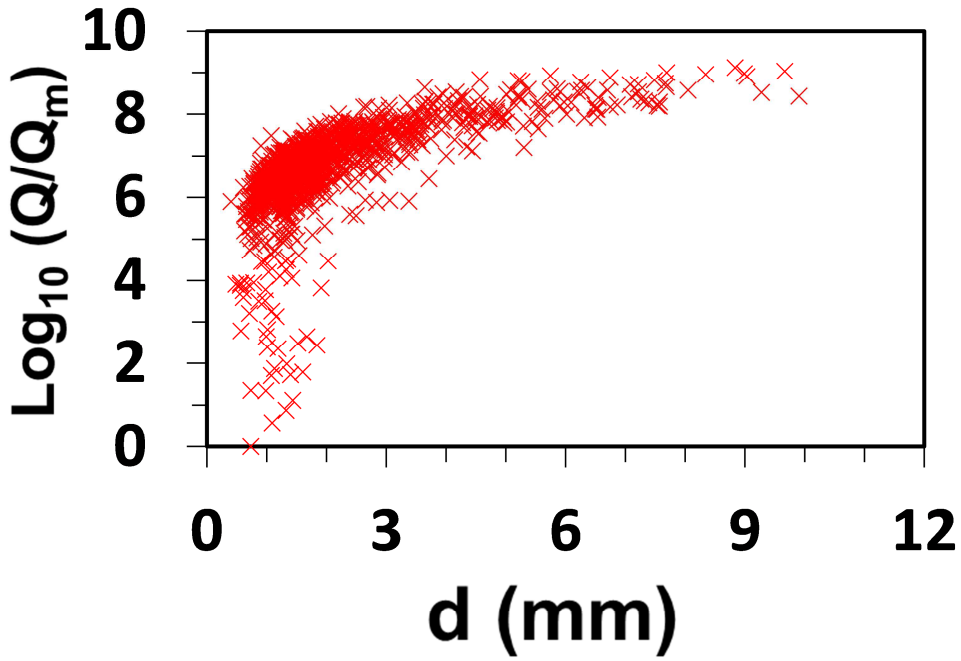

Figure 36. *Q* of each fracture normalized by the minimum value of *Q* of all the fractures in log-10 space plotted against aperture: aperture is proportional to fracture length. Results of one realization shown.

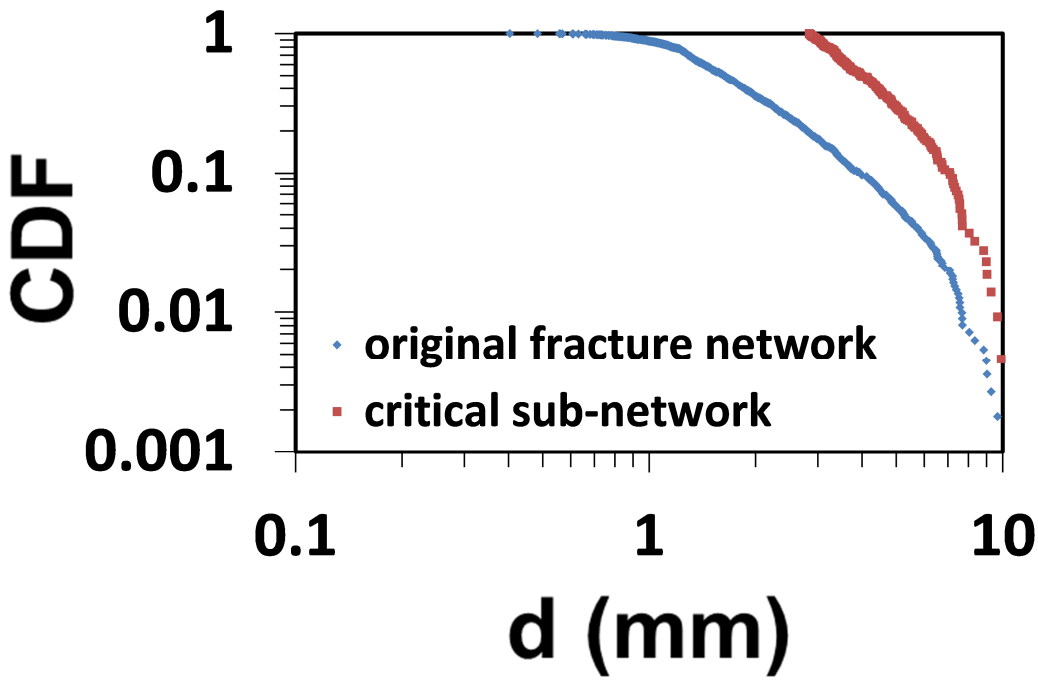

Figure 37. Comparison of aperture distributions of the original fracture network and the critical sub-network: aperture is proportional to fracture length. Results of one realization shown.

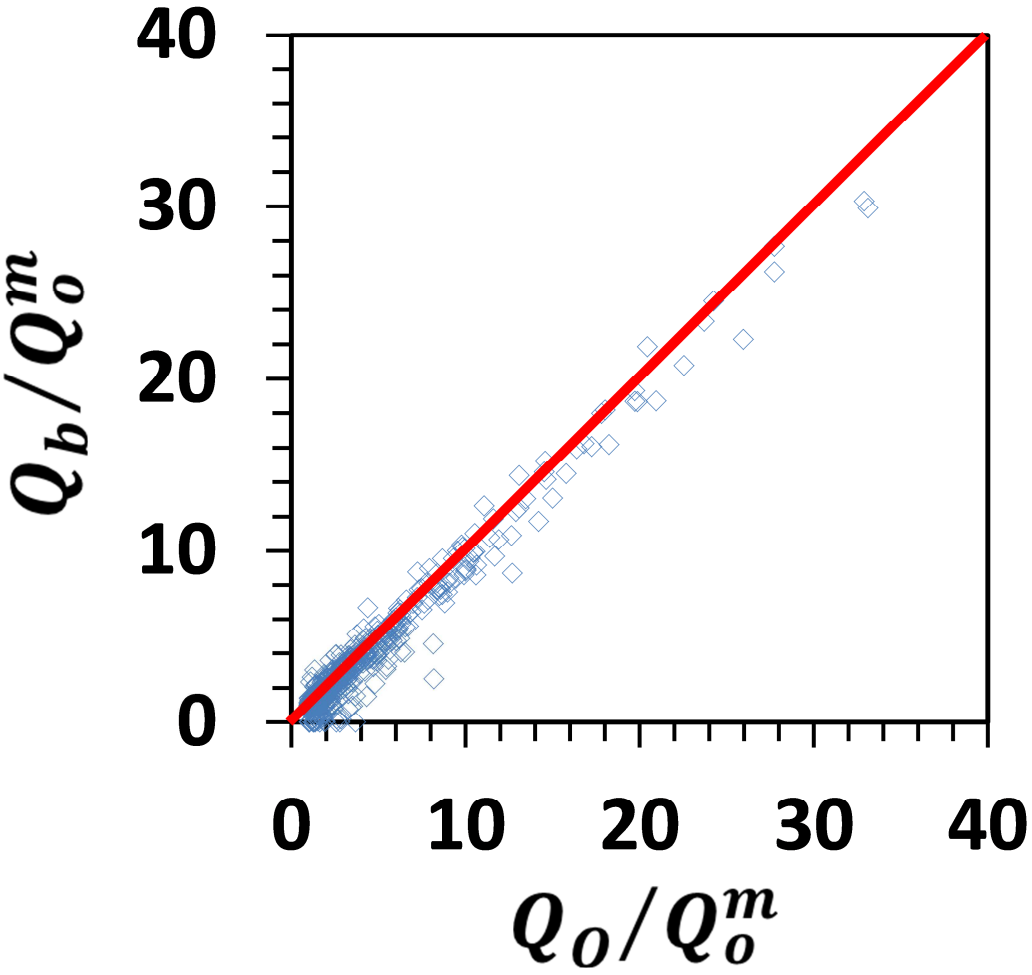

Figure 38. Comparison of Q of fractures when they are in the original fracture network (Q_0) and in the critical sub-network (Q_b): the case of the aperture is proportional to the fracture length. Both of Q_0 and Q_b are normalized by the minimum value of Q in the original fracture network (Q_o^m). Results of one realization shown.

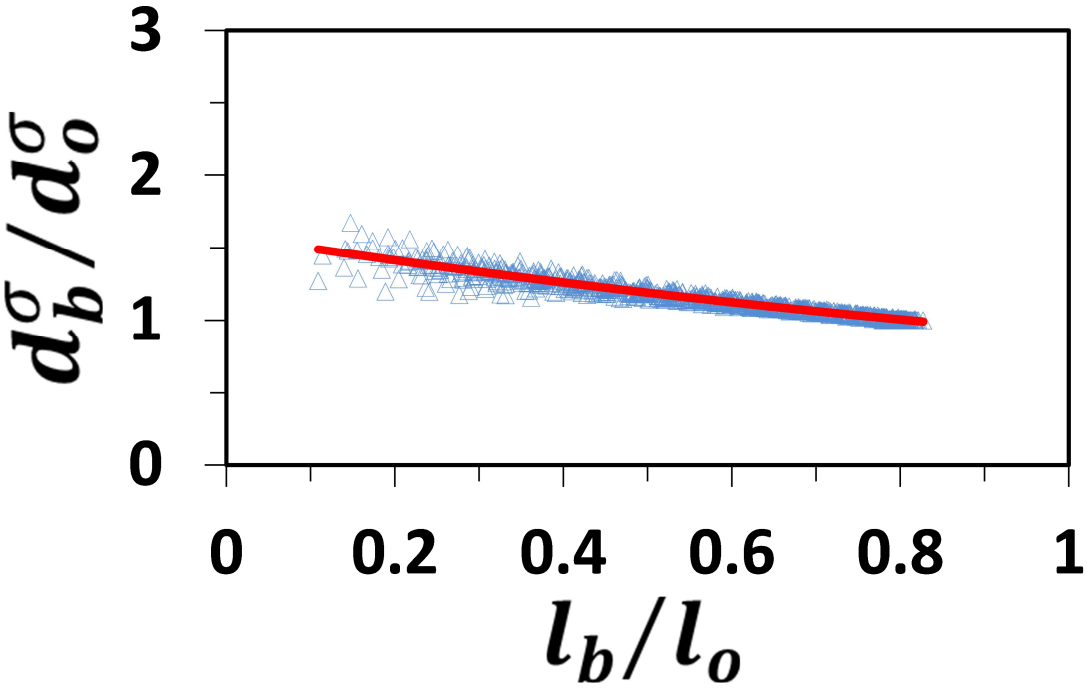

Figure 39. Standard deviation of apertures in the critical sub-network backbone (d_b^σ) normalized by the standard deviation of apertures in the original fracture network (d_o^σ), plotted against the length of the backbone of the truncated fracture network (l_b) normalized by the total length of the original fracture network (l_0): aperture is proportional to fracture length. Results of 100 realizations shown. Red curve is the average trend curve.

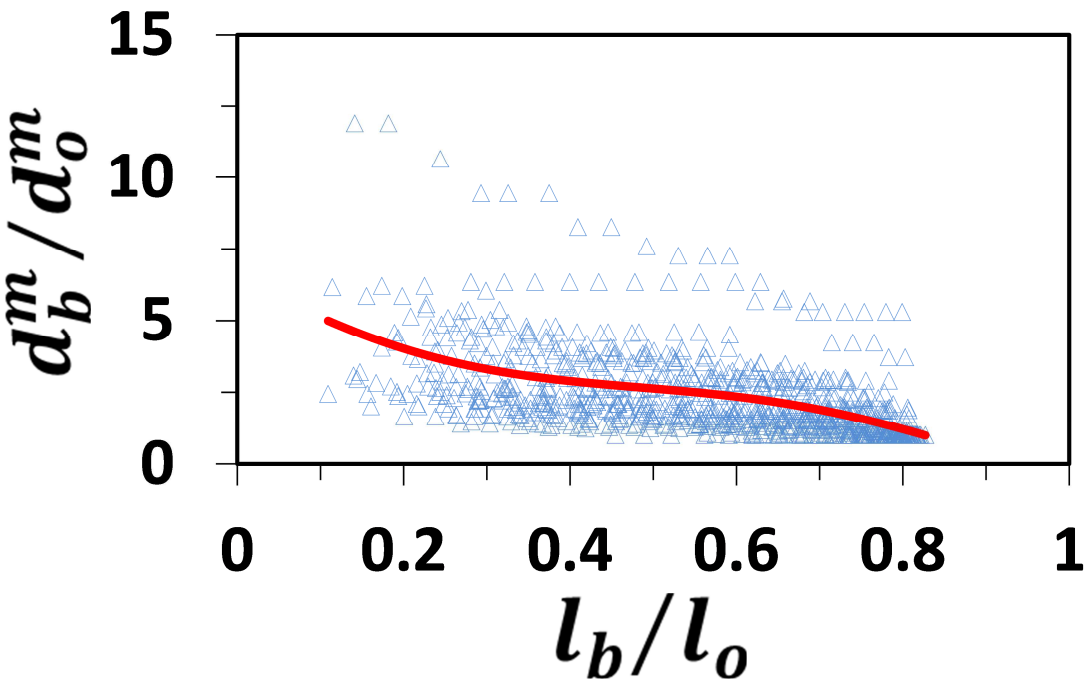

Figure 40. Minimum aperture of the sub-network backbone (d_b^m) normalized by the minimum aperture of the original fracture network (d_o^m)), plotted against the length of the backbone of the truncated fracture network (l_b) normalized by the total length of the original fracture network (l_0): aperture is proportional to fracture length. Results of 100 realizations shown. Red curve is the average trend curve.

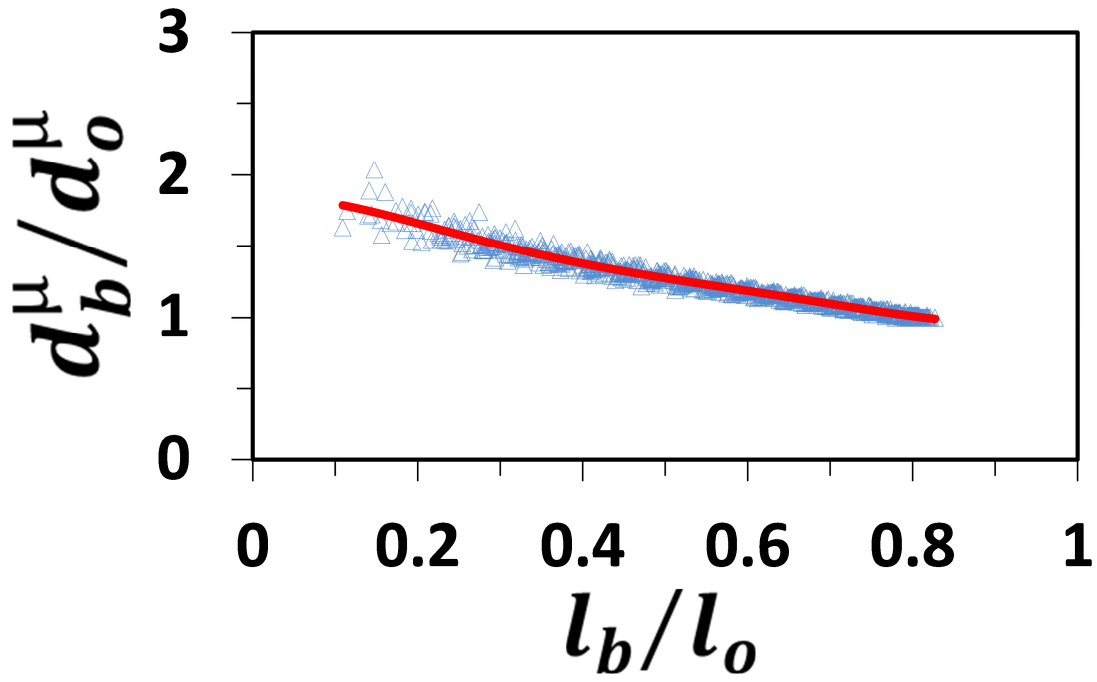

Figure 41. Average aperture of the sub-network backbone (d_b^μ) normalized by the average aperture of the original fracture network (d_o^μ), plotted against the length of the backbone of the truncated fracture network (l_b) normalized by the total length of the original fracture network (l_o): aperture is proportional to fracture length. Results of 100 realizations shown. Red curve is the average trend curve.

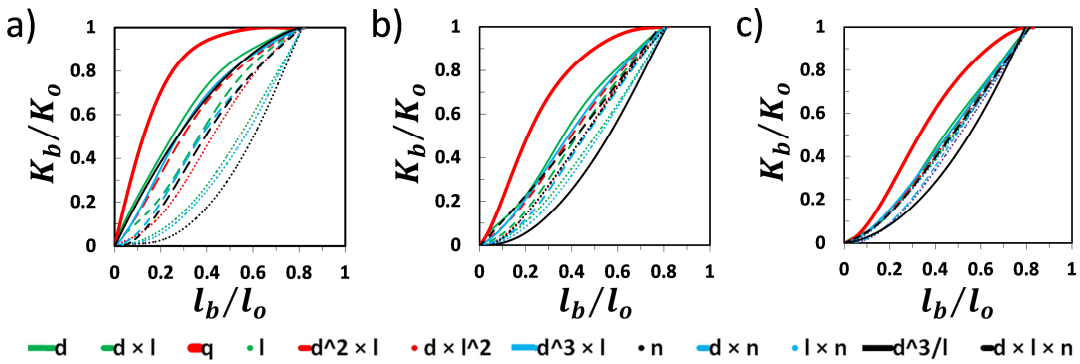

Figure 42. Sub-network equivalent permeability (K) normalized by the equivalent permeability of the original fracture network (K_0), plotted against the length of the backbone of the truncated fracture network (l_b) normalized by the total length of the original fracture network (l_o) for power-law aperture distributions with (a) α = 1.001, (b) α = 2, (c) α = 6. Fractures are eliminated according to different criteria.

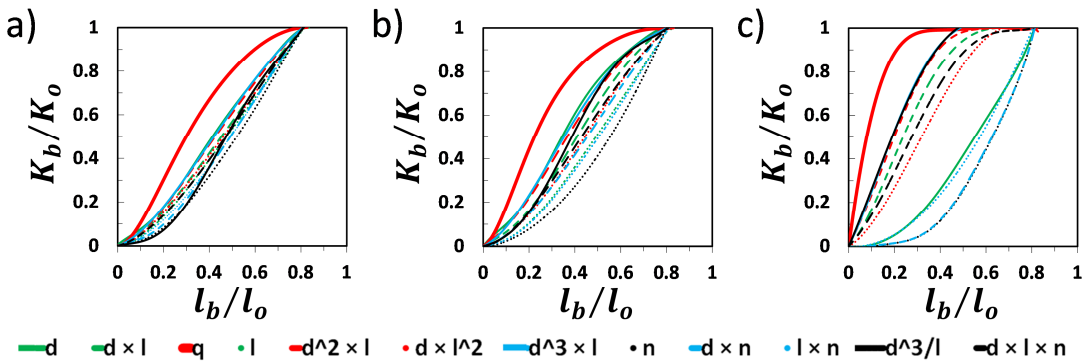

Figure 43. Sub-network equivalent permeability (K) normalized by the equivalent permeability of the original fracture network (K_0), plotted against the length of the backbone of the truncated fracture network (l_b) normalized by the total length of the original fracture network (l_o) for log-normal aperture distributions with (a) σ = 0.1, (b) σ = 0.2, (c) σ = 0.6. Fractures are eliminated according to different criteria.

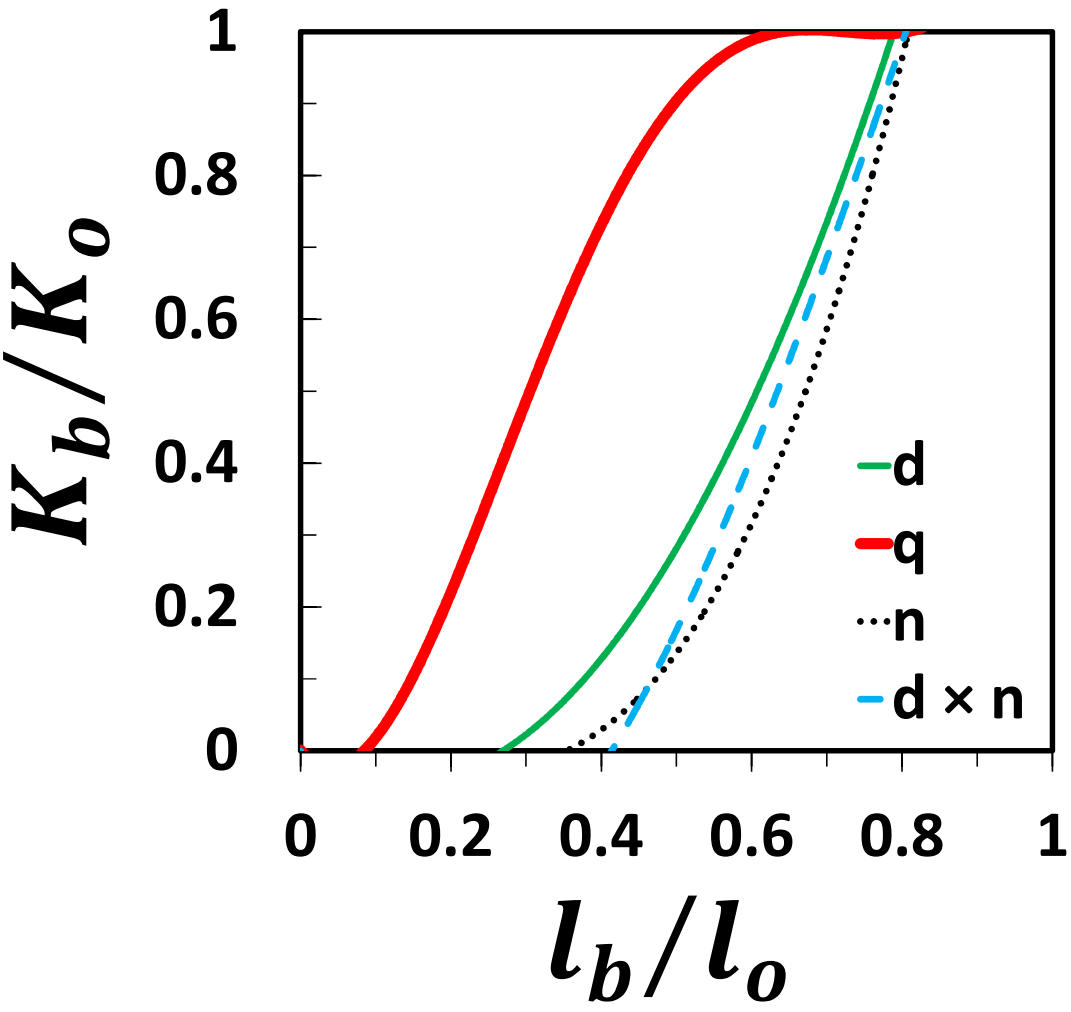

Figure 44. Sub-network equivalent permeability (K) normalized by the equivalent permeability of the original fracture network (K_0), plotted against the length of the backbone of the truncated fracture network (l_b) normalized by the total length of the original fracture network (l_o), for the cases where the aperture is proportional to the fracture length. Fractures are eliminated according to different criteria.

Table 1

Criterion	Description
1	Aperture (d)
2	Length (l)
3	Number of intersections (n)
4	Flow simulation results (q)
5	Aperture × Length ($d \times l$)
6	Aperture^2 × Length ($d^2 \times l$)
7	Aperture^3 × Length ($d^3 \times l$)
8	Aperture × Length^2 ($d \times l^2$)
9	Aperture^3 / Length (d^3 / l)
10	Aperture × Number of intersections ($d \times n$)
11	Length ×Number of intersections ($l \times n$)
12	Aperture × Length × Number of intersections ($d \times l \times n$)